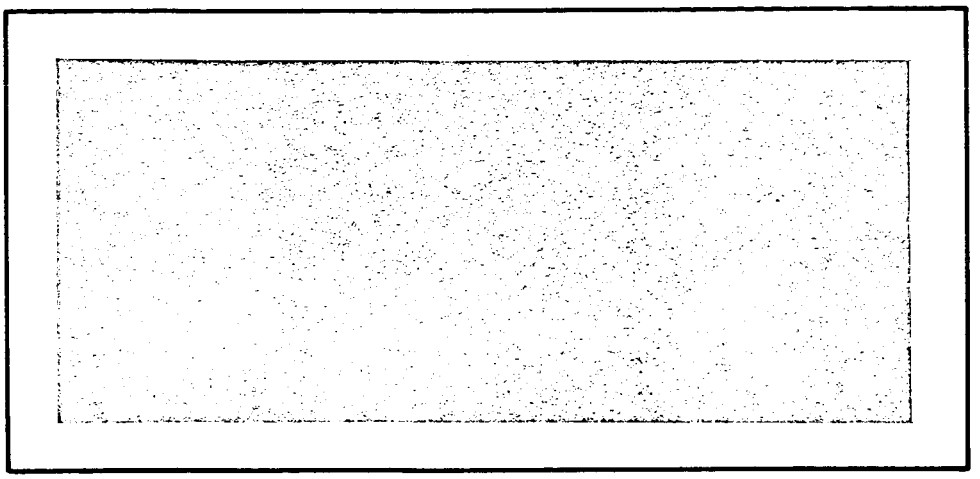

SCIENCE APPLICATIONS, INC.

(NASA-CR-161100) LONG-TERM RISK ANALYSIS ASSOCIATED WITH NUCLEAR WASTE DISPOSAL IN SPACE (Science Applications, Inc., Schaumburg, Ill.) 93 p

N79-74674

Unclas
00/73 14357

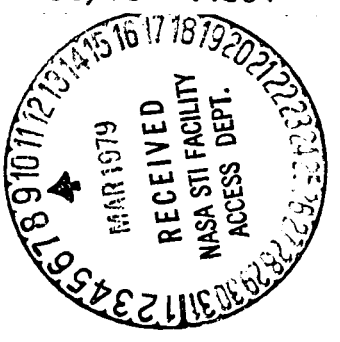

Long-Term Risk Analysis Associated with Nuclear Waste Disposal in Space

Science Applications, Inc, Schaumburg, IL

Prepared for

National Aeronautics and Space Administration
Huntsville, AL

Dec 78

Report No. SAI 1-120-062-T12

LONG-TERM RISK ANALYSIS ASSOCIATED WITH NUCLEAR WASTE DISPOSAL IN SPACE

by

Alan L. Friedlander
Donald R. Davis

Science Applications, Inc.
1701 East Woodfield Road
Schaumburg, Illinois 60195

for

NASA-George C. Marshall Space Flight Center,
Alabama 35812

Contract No. NAS8-33022

December 1978

FOREWORD

This technical report is the final documentation of all work performed by Science Applications, Inc. for NASA/Marshall Space Flight Center under Contract No. NAS8-33022. The period of performance covers April-December 1978. Analysis methods and results presented herein are intended to assist NASA and DoE planners in assessing the viability of space disposal concepts within the overall context of nuclear waste management.

The authors express their appreciation to the following who provided valuable assistance in areas of technical discussion, data sources and report preparation: Gene Austin, NASA/MSFC Contract Monitor; Bob Nixon, NASA/MSFC; Jim Williams, JPL; Terri Ramlose and Kathy Osadnick, SAI Chicago Office.

TABLE OF CONTENTS

LIST OF FIGURES

LIST OF FIGURES (cont'd.)

LIST OF TABLES

LONG-TERM RISK ANALYSIS ASSOCIATED WITH NUCLEAR WASTE DISPOSAL IN SPACE

1. INTRODUCTION AND SUMMARY

Extraterrestrial disposal of hazardous waste material is being considered by NASA and DoE planners as a potential augmentation option of the national program for nuclear waste management. In support of this program planning effort, the present study addresses one aspect of the problem quite relevant to decision-making, namely, a quantitative measure of future risk and risk reduction requirements associated with the unplanned event of Earth reentry. Such an event, although rare, could result from either a failure occurrence in the deployment propulsion system or long-term instability of a nominal storage orbit.

The work reported herein is a continuation and logical extension of previous studies concerned with risk analysis [1,2]. These earlier investigations examined disposal destinations in heliocentric space and Earth-Moon space and were comprised of the following topical scope: (1) performance analysis of disposal options; (2) deployment accuracy and reliability; (3) orbit stability; (4) planetary encounter/Earth reentry probability; (5) long-term integrity of heat shield/containment materials; and (6) health consequences of unprotected reentry.

With continuing in-house studies at MSFC [3], and their support contractors Battelle Columbus Labs [4] and Science Applications, Inc., a higher level of maturity has evolved in defining preferred disposal options and requirements. The current baseline concept would have waste payloads delivered to a stable solar orbit in the region between Venus and Earth; an alternate region of stability lies between Earth and Mars. Analytic, quantitative data that has previously been presented on questions of orbit stability and Earth reentry risk are thought to be basically correct. However, as the space disposal concepts mature, it is important that this data be verified by more sophisticated (accurate) methods such as numerical integration and Monte Carlo statistical experiments. The present study then addresses this need for further verification analyses.

1.1 Study Objectives and Scope

Three specific task areas of investigation were defined as described below.

Task 1: Validation of Solar Orbit Stability. The objective of this task is to verify the quantitative bounds on the long-term ($\sim 10^6$ years) stability of candidate storage orbits that were previously derived using secular perturbation theory. These orbits are initially circular and span the range 0.83 to 0.88 AU between Venus and Earth, and 1.17 to 1.19 AU between Earth and Mars. The verification analysis is concerned with evaluating the short-period perturbation effects which are ignored in the secular theory, and evaluating the analytical solution of the secular theory. This may be accomplished by numerical integration in the following manner: (1) short-term integration of the full equations of motion; and (2) long-term integration of the complete averaged equations of motion. Both methods are examined in terms of accuracy and computation time tradeoffs. Numerical tests are performed for candidate storage orbits and stability results compared with those of secular theory.

Task 2: Validation of Earth Reentry Risk. The objective of this task is to verify the quantitative probabilities of planetary collision, and in particular Earth reentry, for "failed" payloads in solar orbit for time periods up to 5×10^6 years. Previous results were derived using Öpik's theory of planetary encounters to determine the orbit-conditional event probabilities which were then integrated over the deployment system failure distribution to obtain the overall risk profile. The new methodology uses a Monte Carlo simulation of orbital evolution resulting from close planetary approaches to generate collision statistics as a function of time. Revised orbit-conditional event probabilities are obtained in this manner. The Monte Carlo procedure supersedes the "averaging" approach inherent to Öpik's theory and presumably yields a more accurate statement of risk. A sufficiently large number of runs are made to generate statistical data for direct comparison with previous results. Revised risk profiles including retrieval (rescue) options are prepared as necessary.

Task 3: Rescue Mission Requirements. The objective of this task is to evaluate the ΔV and propulsion stage requirements to carry out rescue missions (retrieval and placement) for a failed payload in solar orbit. The feasibility and requirements of automated rendezvous/docking in deep space are also assessed.

It should be noted that the scope of the present study deals with the long-term aspects of risk assessment, i.e., failure events which occur after injection to deep space. It does not encompass systems failures and abort situations during the launch-to-orbit phase nor that portion of the early deployment phase while the payload is still in Earth orbit. These near-term failure modes are obviously important in the overall analysis of deployment safety and they are being treated in concurrent studies at MSFC and Battelle Columbus Labs.

Results of this study are summarized briefly in the following subsection. Organization of the main sections of the report follows the task sequence described above. Each section is independent for the most part and may be read separately in any order.

1.2 Summary of Results

Solar Orbit Stability. Numerical integration of the full equations of motion for time periods up to 12,000 years was performed for presumably stable orbits between Earth and Venus. The results indicate that secular perturbation theory is certainly valid ($\leq 10^{-3}$ AU error) for time scales of order 10^4 years and probably valid for much longer intervals. The stability prediction of the analytic secular theory was then tested by numerically integrating the complete averaged equations of motion for time periods up to 500,000 years. Figure 1-1 shows the orbit evolution comparison between analytic and numerical secular theory. The agreement is very good in terms of the heliocentric distances covered and the general behavior of the orbital history. The increasing phase difference between the two cases is attributed to the truncation of higher order terms in formulation of the

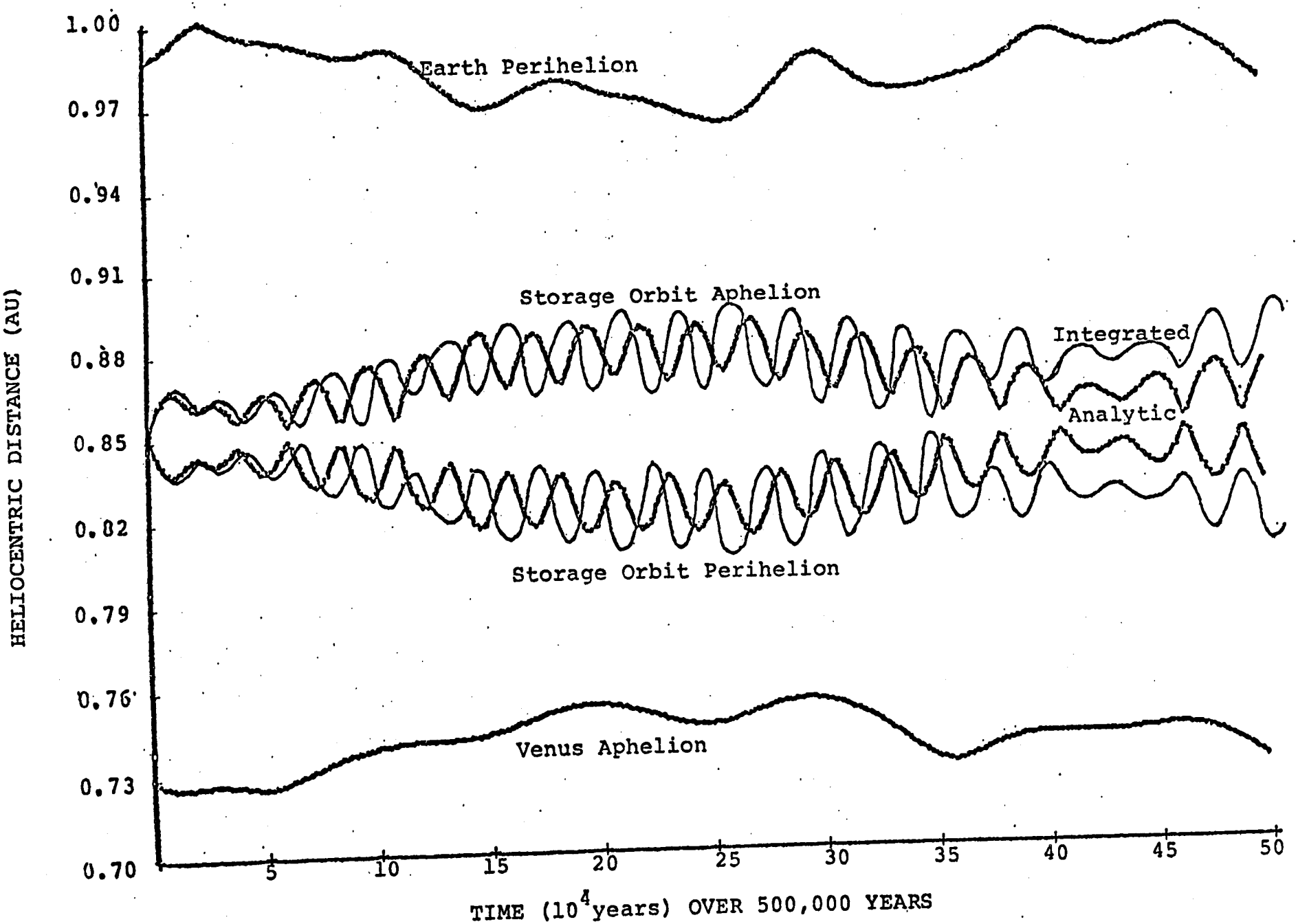

FIGURE 1-1 COMPARISON OF ORBIT VARIATIONS BASED ON ANALYTIC SECULAR THEORY (heavy lines) AND INTEGRATED AVERAGED EQUATIONS (thin lines).

analytic theory. Similar results were found for an initially circular orbit at 1.19 AU. One interesting byproduct of the integration tests was the discovery of the possibly destabilizing effect of near-resonant orbits. The nominal 0.86 AU orbit is quite close to the 5:4 commensurability with Earth's orbital period, this occurring at a = 0.86177 AU. It would perhaps be best to select a new nominal target orbit that is slightly removed from this resonance, e.g., at 0.85 AU distance. Further work is recommended on the question of near-resonant orbit effects. As a general conclusion of the verification analysis, storage orbits between Venus and Earth or between Earth and Mars give every indication of meeting the desired stability requirements for waste disposal, i.e., for time scales of the order 10^6 years. The definitive test would, of course, involve numerical integration of the complete equations of motion for this period of time--a rather expensive research undertaking. However, it is suggested that this be done as soon as practical.

Earth Reentry Risk. Analytic theory predictions of the long-term probability of Earth collision (resulting from deployment system failures) has been verified to within a close order-of-magnitude. A fortuitous result is that the Monte Carlo data, presumably more accurate, indicate a lower risk by a factor of $\sim$5 for solar storage orbit missions. Figure 1-2 shows a comparison of the analytic and numerical probability distributions for the nominal 0.86 AU destination orbit assuming a 99% reliability level for the deployment propulsion system. The revised results show that the reentry probability, for a single payload launch without rescue capability, is 6.4×10^{-4} for $T \leq 10^5$ years, 2.2×10^{-3} for $T \leq 10^6$ years, and 5.7×10^{-3} for $T \leq 10^7$ years. Quite similar results are obtained for the solar orbit mission at 1.19 AU. Mission planners, quite understandably risk-adverse, have stated that a much smaller reentry probability of order 10^{-8} might be acceptable. This means, for example, that in a total space disposal program comprising 100 launches, there is only one chance in a million that any payload will reenter Earth's atmosphere within a time interval of order 10^6 years after launch. It appears that the only

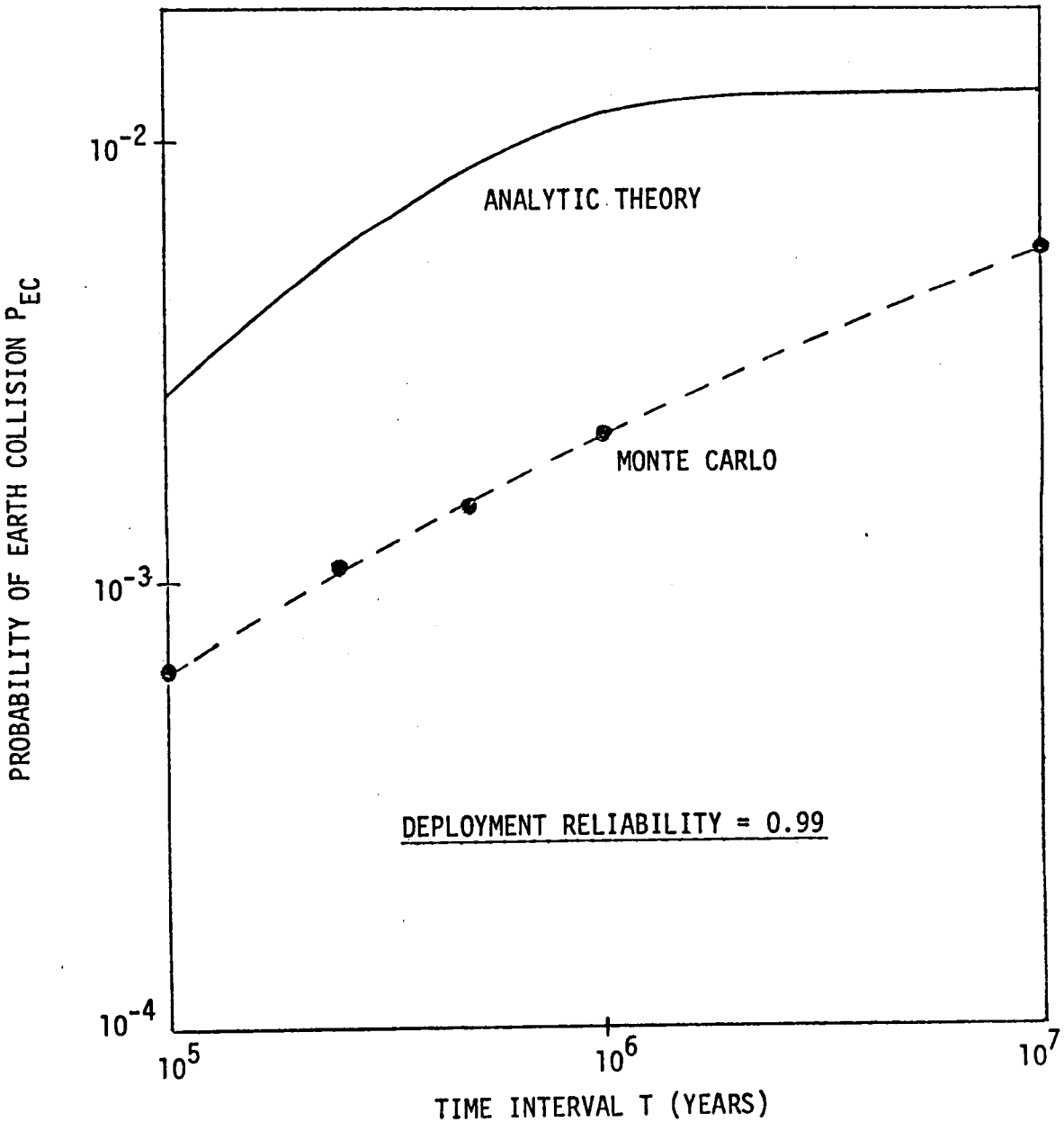

Fig. 1-2 COMPARISON OF ANALYTIC AND MONTE CARLO PREDICTION OF EARTH REENTRY RISK FOR SOLAR ORBIT MISSION (r = 0.86 AU, $i = 2^o$)

practical way to assure such low risk is through rescue mission capability. Figure 1-3 presents the revised 10^6 year risk profile for the 0.86 AU storage orbit; the effects of system reliability (R) and rescue mission degree of redundancy (N) are shown parametrically following the relationship $P(R,N) = P(R,0)(1 - R)^N$. For example, with R = 0.99, each additional rescue mission yields 2 orders-of-magnitude further reduction in collision probability. The 10^{-8} risk level can be attained with two rescue missions if the reliability is 0.996, or at most four rescue mission attempts if the reliability is only 0.965.

Rescue Mission Requirements. A failed payload in solar orbit can be retrieved and placed into a stable orbit using the same propulsion hardware (OTV and kick stage*) employed for the nominal payload deployment. However, since the ΔV budget associated with rescue operations is always larger than nominal, it may be necessary in many instances to utilize two baseline kick stages. A possible alternative option is also available wherein a single kick stage is utilized to recover a stable orbit slightly different than the nominal target orbit. Table 1-1 presents one example from the range of failure cases studied. In all cases, the rescue mission is launched within one year of the nominal payload launch date (T_L), and stable orbit placement occurs within five years of that date. An important assumption apropos to the analysis is that the failed kick stage be jettisoned after rendezvous; it would be very inefficient to have to carry this dead weight through orbit transfer maneuvers. The most critical aspect of rescue missions is undoubtedly the ability to rendezvous and dock with a payload in deep space. The preliminary assessment made here is that automated operations are technically feasible based on current technology if a cooperative rendezvous mode can be assured. Such assurance implies a limited time interval between nominal payload launch and retrieval, and probably some degree of redundancy in payload vehicle systems (attitude control and communications) to enhance operational reliability. Some of the key features and requirements of rescue operations are summarized in Figure 1-4.

*Kick stage (also referred to as SOIS - Solar Orbit Insertion Stage) is required for circularization burn at 0.86 AU on nominal mission.

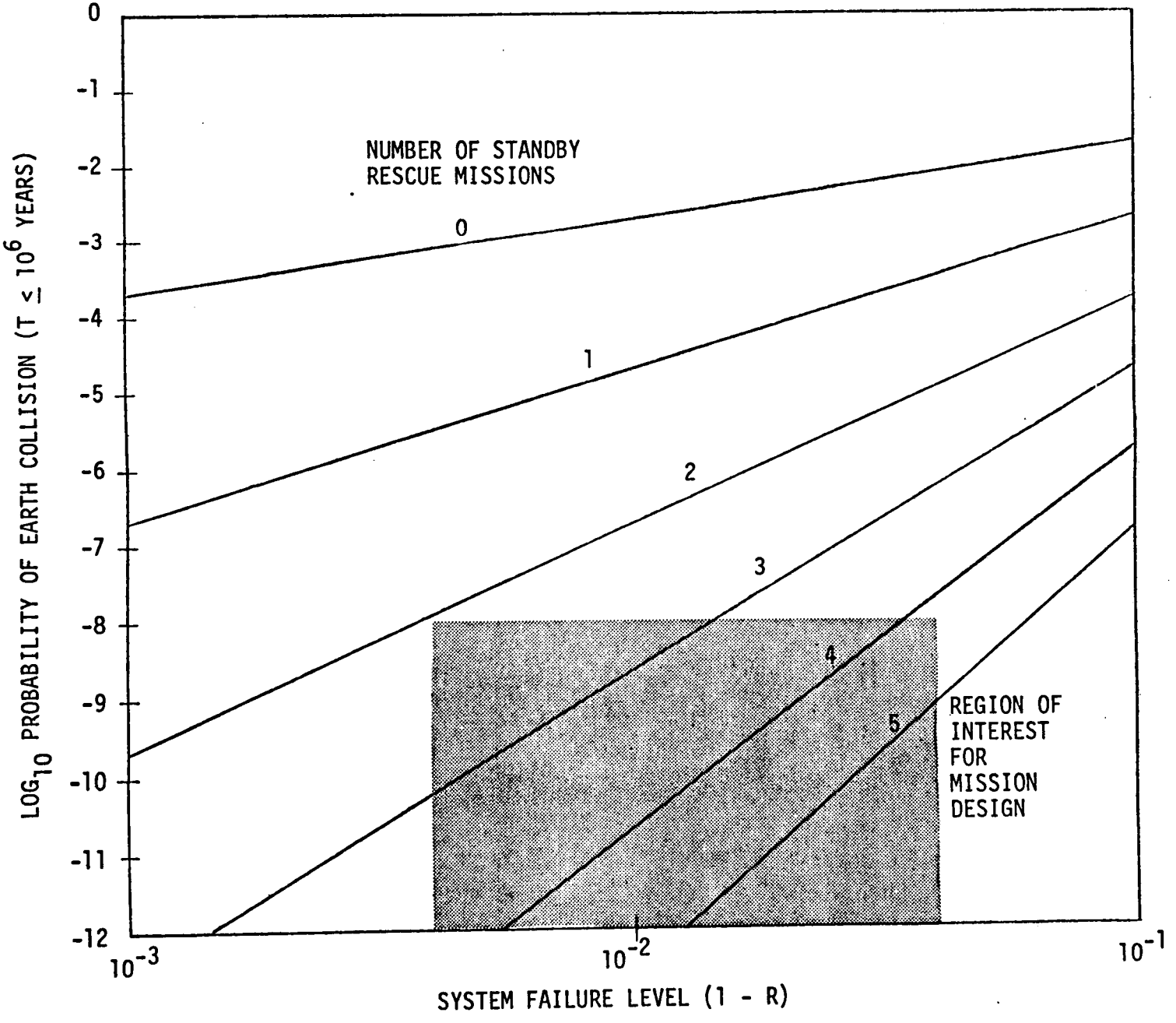

Fig. 1-3 10^6 YEAR RISK PROFILE FOR SOLAR ORBIT DISPOSAL WITH RESCUE CAPABILITY, NOMINAL ORBIT: 0.86 AU CIRCULAR, 2^o INCLINATION

Table 1-1

RESCUE MISSION PROPULSION REQUIREMENTS - CASE STUDIES

CASE NUMBER: 2B (Placement at T_L + 4.240^y)

FAILURE EVENT: OTV and kick stage failure at T_L
Payload in orbit 0.93 × 1.0 AU, I = 2°

RESCUE RESPONSE: Launch two* baseline kick stages for rendezvous, transfer and placement 0.86 AU circular

RESCUE SCENARIO:

Event	Time	Distance	C_3 or ΔV
Inject to 0.906 × 1.0 AU orbit	T_L + 1.0^y	1.0 AU	C_3 = 1.61 @ I = 2°
Wait three revolutions			
Rendezvous and dock	T_L + 3.792^y	1.0	ΔV = 0.295 km/sec
Transfer to 0.86 × 1.0 AU	T_L + 3.792^y	1.0	0.598
Placement	T_L + 4.240^y	0.86	1.187

STAGE REQUIREMENTS:

Stage Number	ΔV (km/sec)	Propellant (lbs)
1 (Baseline Kick)	0.893	8829 (8397 used)
2 (Baseline Kick)	1.187	8829 (7591 used)

TOTAL INJECTED WEIGHT: 2 × 11943 = 23886 lbs to C_3 = 1.61

TOTAL RESCUE MISSION TIME: 3.240 years

*Alternative using only single kick stage is placement into circular orbit 0.888 × 0.888 AU, or elliptical orbit 0.86 × 0.917 AU.

Fig. 1-4

AUTOMATED RENDEZVOUS AND DOCKING IN SOLAR ORBIT

- PREVIOUS EXPERIENCE
  - PRACTICAL IMPLEMENTATION BY SOVIETS IN EARTH-MOON SPACE
  - ANALYSIS AND DESIGN BY U.S. (MANNED PROGRAM, MARS SAMPLE RETURN)

- MOST SIGNIFICANT FEATURES
  - SOME LEVEL OF COOPERATION BY TARGET VEHICLE--OTHERWISE, NEW TECHNOLOGY REQUIREMENTS ASSESSED VERY DIFFICULT
  - HIGH ACCURACY TERMINAL GUIDANCE BY RESCUE VEHICLE
  - ADEQUATE WEIGHT MARGIN FOR RESCUE VEHICLE TO ACCOMMODATE GUIDANCE SYSTEM AND NON-OPTIMUM MANEUVERS

- HIERARCHY OF TARGET VEHICLE OPERABLE SYSTEMS
  - ATTITUDE CONTROL
  - COMMUNICATIONS LINK (COMMAND AND TRACKING)
  - LOW LEVEL MANEUVERABILITY

- RESCUE VEHICLE SYSTEMS
  - LONG RANGE ACQUISITION RADAR
  - SHORT RANGE RF OR SCANNING LASER RADAR
  - CELESTIAL AND INERTIAL ATTITUDE SENSORS
  - AXIAL AND LATERAL THRUSTERS
  - COMMAND SEQUENCER/COMPUTER

Section 1 References

1.1 Friedlander, A. L., et al., "Aborted Space Disposal of Hazardous Material: The Long-Term Risk of Earth Reencounter," Science Applications, Inc., Report No. 1-120-676-T8, February 1977.

1.2 Friedlander, A. L., et al., "Analysis of Long-Term Safety Associated with Space Disposal of Hazardous Material," Science Applications, Inc., Report No. 1-120-676-T11, December 1977.

1.3 NASA/MSFC, "Nuclear Waste Management (Space Option) - Mission and Design Analysis," January 1979.

1.4 Battelle Columbus Laboratories, "Evaluation of the Space Disposal of Nuclear Waste - Phase II," NASA Contract NAS8-32391, January 1979.

2. VALIDATION OF SOLAR ORBIT STABILITY

2.1 Background

The extraterrestrial option for the storage of nuclear wastes requires orbits that are known to be stable, i.e., do not cross or come close to the orbit of any planet for a time interval around 500,000 years, which would allow long-lived radionuclides to decay through many halflives. Such an interval is very long when compared with orbit lifetime requirements for most manmade satellites, typically only a few years or decades. However, the 5×10^5 year interval is comparable to the longest period variation in the eccentricity of planetary and asteroid orbits while it is short compared with the orbital lifetime of planet-crossing asteroids and comets in the inner solar system (10^7 to 10^8 years). In an earlier study (Friedlander et al. [1]), the theory of secular perturbations for small bodies, originally developed for investigations of the long-term motion of the asteroids, was applied to investigate the stability of various orbits initially located in the "gaps" between the terrestrial planets. The method of secular perturbations requires that the short period perturbations of the orbit be eliminated by averaging over position in the perturbed orbit and the perturbing body's orbit. Analytic solutions for the orbit evolution can be obtained if the averaged equations are truncated after first order in the disturbing mass and second order in the eccentricities and inclinations (Brouwer and Clemence [2], Brouwer [3]). The resulting equations of motion reduce to a system of coupled, linear equations. This theory was used to determine the range of semimajor axes (a) between Earth and Venus and between Earth and Mars, for which initially nearly circular orbits would be stable in the sense of avoiding neighboring planetary orbits for intervals of 500,000 years. The interplanetary gap between Venus-Earth and Earth-Mars together with the orbital evolution for representative orbits is given in Figures 2-1 and 2-2, taken from the earlier study. These initially circular orbits at 0.86 and 1.19 AU with 2.0° initial inclination are adopted for now as nominal storage orbits.

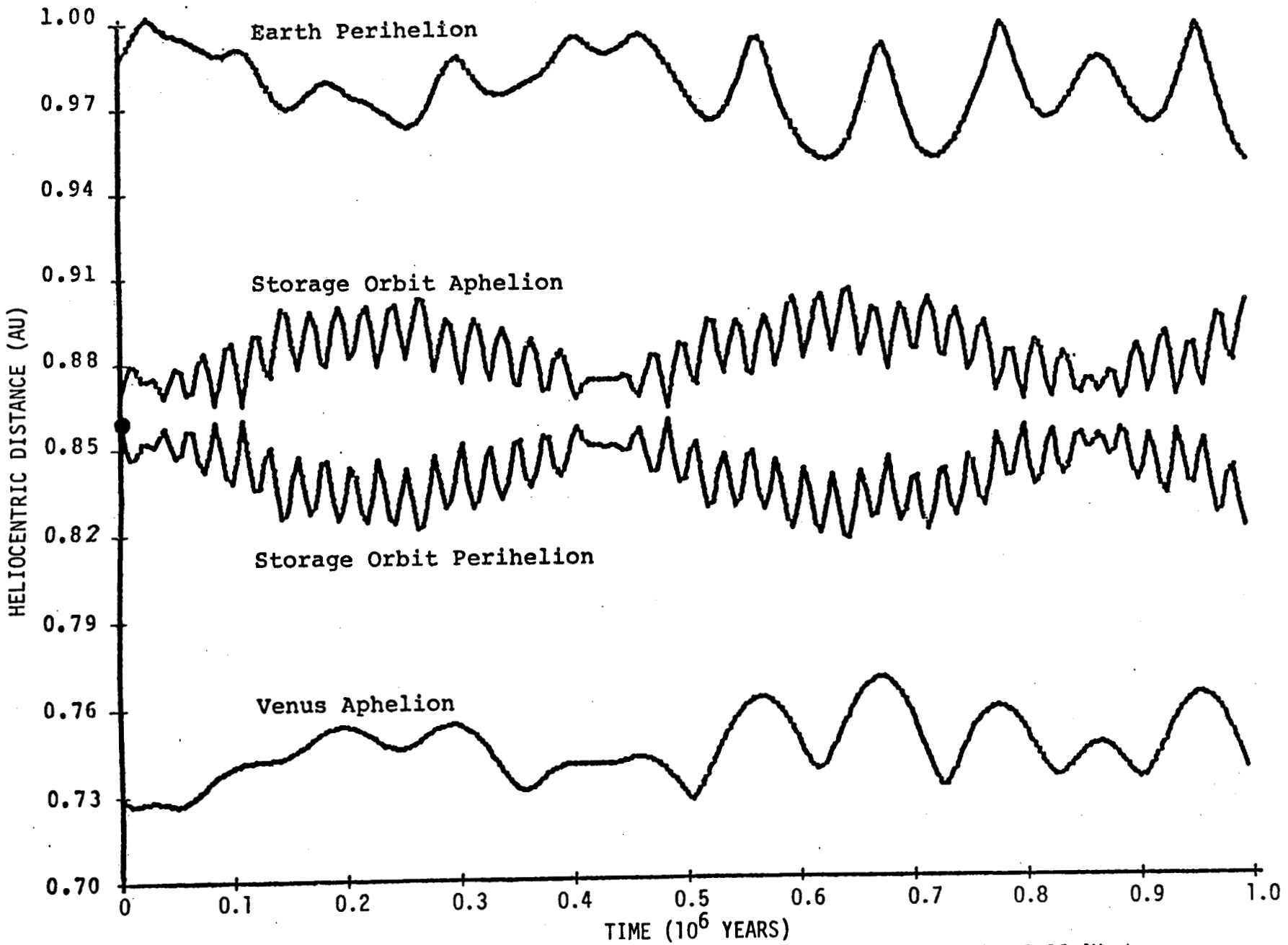

Fig. 2-1 ORBITAL VARIATIONS OF AN INITIALLY CIRCULAR ORBIT AT a = 0.86 AU

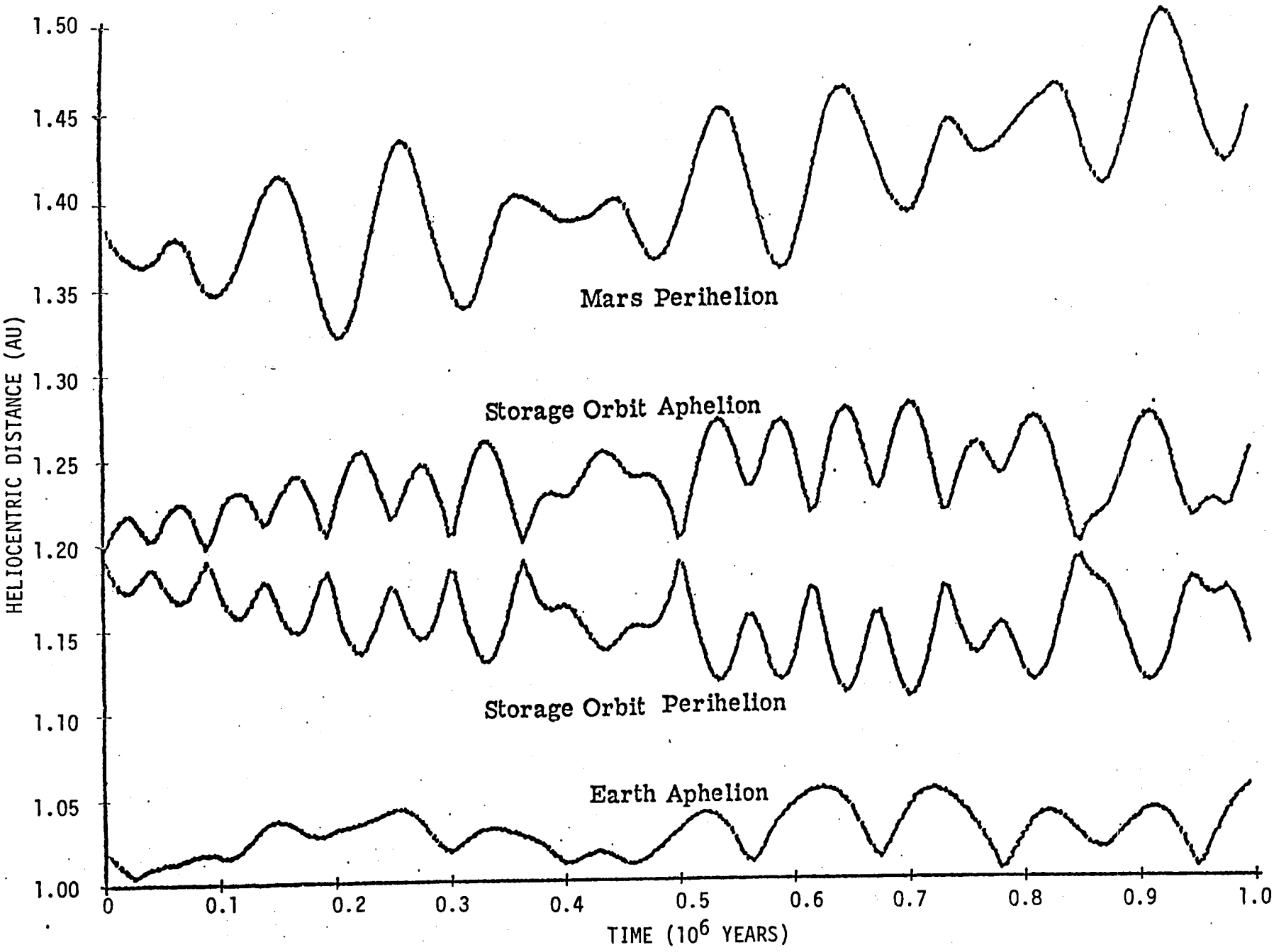

Fig. 2-2 ORBITAL VARIATIONS OF AN INITIALLY CIRCULAR ORBIT AT a = 1.19 AU

The use of secular perturbation theory is necessary to survey many potential storage orbits over long intervals; however, there are various approximations made in the theory as well as restrictions on the applicability of the theory itself which give rise to questions regarding the accuracy of the analytic solution. Secular perturbation theory has been applied to studying the long-term motion of the planets and was given a partial vote of confidence by numerical integration. While the most recent analytic secular perturbation solution for the solar system (Brouwer and Van Woerkom [4]) includes all planets save Pluto, the numerically integrated comparison by Cohen et al. [5] treated only the outer planets, Jupiter through Neptune. The inner planets were included only by the device of "casting them into the Sun," i.e., augmenting the Sun's mass by the mass of the terrestrial planets. In general, the agreement between secular theory and numerical integration was quite good with the principal discrepancies arising in the behavior of Uranus and Neptune. This discrepancy is probably due to Brouwer and Van Woerkam's ignoring terms in the analytic expansion which would account for the near 2:1 communsurability between Uranus and Neptune. Their secular theory neglects such resonance effects. No confirming numerical studies have been undertaken for terrestrial planets nor for application of secular perturbations to small bodies; however, there has not been any reason to doubt the secular results as long as resonances are avoided. Clearly, though, when orbits are being proposed for storage of nuclear wastes, it must be demonstrated that the stability analysis is valid.

This study sought to confirm results from secular theory by numerical integration. Direct integration of the full equation of motion for a body in the inner solar system over a timescale of 10^5 to 10^6 years is an expensive undertaking. A review of the literature of long-term integrations indicates that timescales of order 10^6 years have been covered, but only for the outer planets where the orbital periods are much longer. The integration of the outer planets to confirm secular theory covers 10^6 years,

or 8.4×10^4 orbits of Jupiter. Other integrations such as the 4.5×10^6 year integration of Pluto (Williams and Benson [6]) span only 1.4×10^4 revolutions of Pluto. In the inner solar system, integrations cover roughly the same number of orbits, but give a shorter integration interval due to the shorter orbital periods, e.g., the orbit of asteroid 1685 Toro was integrated for 5000 years (3125 orbital periods of Toro). An orbit between Earth and Venus with a = 0.86 AU has a period of nearly 0.8 years; hence, a 500,000 year integration would require nearly 6.3×10^5 orbits, nearly an order of magnitude greater than has been done before. For this validation study, a two-part approach was adopted: first, to numerically integrate over a 500,000 year interval the complete averaged equations of motion to find the effect on the analytic solution of truncating higher order terms in the orbit elements. The second part consists of numerically integrating the full equations of motion over as long an interval as possible given the available resources.

2.2 Numerical Integration Program

The integrations were performed using an integration program originally developed by J. G. Williams for studying the long-term motion of planets and asteroids. This program has the capability of integrating both the full equations of motion and the averaged equations of motion, including higher order terms neglected in the analytic solution. The program calculates the evolution of a non-resonant, non-intersecting orbit, which is perturbed by any of the planets Mercury through Neptune. Since we are interested in long-term behavior, the planetary orbits cannot be treated as fixed, but rather the orbital changes due to their mutual perturbations must be included. The Brouwer-Van Woerkom solution for the orbits of the eight principal planets is incorporated into the model. The program integrates the desired formulation for the variation of the orbit elements using a fourth order Runge-Kutta algorithm with either fixed stepsize or variable stepsize to keep the changes in any desired orbit element within specified bounds. The program presently is operational

on the JPL Univac 1108 and performs integrations with double precision arithmetic, giving about 17 decimal digits of precision. The program takes about 0.1 CPU seconds per integration step of the full equations of motion when all perturbing planets are included.

The long integration times dictate that compromises be made between integration accuracy and running time. Accuracy is improved by using smaller stepsizes, but smaller stepsizes require longer execution times to cover the same interval. Several runs were made over intervals of up to 2000 years for the full equations of motion and to 5000 years for the averaged equations to find the largest stepsize which does not incur a significant loss of accuracy. Table 2-1 compares the eccentricity from integrations of the full equations case with different stepsizes. Timesteps of the order of the orbital period or larger give results considerably different from short timestep runs, while there is little difference between the five-day and 0.05 year stepsize runs, and the 0.1 year and 0.05 year cases are in reasonably good agreement. The significant loss of accuracy occurs for stepsizes greater than 0.1 years--clearly the 1 year stepsize is too large. Hence, 0.1 years seems the best stepsize for long-term integration of the full equations. Comparison of integration using this fixed stepsize with the variable step with $\Delta e_{max} = 3 \times 10^{-5}$ shows no significant loss of accuracy; the fixed stepsize case ran about twice as fast.

For integration of the averaged equations of motion, the timestep can be considerably longer since we are no longer concerned with short period variations. The timestep can be longer than the orbital period, but should be small compared with the timescale of significant changes in the orbital elements. A series of 5000 year runs was undertaken to determine the maximum timestep without significant accuracy loss; the results of this investigation are summarized in Table 2-2. Only stepsizes longer than 100 years are not acceptable while the 1 year step buys little additional accuracy relative to a 10 year stepsize. The desired best stepsize is in the range of 10 to 100 years. Timing tests indicate a 500,000 year

TABLE 2-1: ECCENTRICITY COMPARISON USING FULL EQUATIONS OF MOTION WITH DIFFERENT STEPSIZES

Initial orbit: $a = 0.86$ AU, $e = 1 \times 10^{-5}$, $i = 2.0^{\circ}$

Time After Epoch (years)	Stepsize (years) 1	.1	variable $\Delta e_{max}=3\times10^{-5}$	.05	5 Days
A) Long Term Integration					
0	1×10^{-5}	1×10^{-5}	1×10^{-5}	1×10^{-5}	1×10^{-5}
500	.00474	.00328	-	-	-
1000	.01141	.00410	-	-	-
1500	.02150	.00759	-	-	-
2000	.02625	.00870	-	-	-
B) Intermediate Term					
50	-	.00075	.00058	.00066	
100	-	.00127	.00129	-	
150	-	-	-	-	-
200	-	.00203	.00204	-	-
C) Short Term					
5	-	.000397	-	.000464	.000472
10	-	.000687	-	.000741	.000748
15	-	.00105	-	.00108	.00109
20	-	.00140	-	.00138	-
25	-	.00136	-	.00132	-
30	-	.00139	-	.00134	-
35	-	.00145	-	.00138	-
40	-	.00111	-	.00102	-
45	-	.00085	-	.00076	-
50	-	.00075	-	.00066	-

TABLE 2-2: ECCENTRICTY COMPARISON USING AVERAGED EQUATIONS WITH DIFFERENT STEPSIZES

Initial orbit: $a = 0.86$, $e = 1 \times 10^{-5}$, $i = 2.0^{o}$

Time After Epoch (years)	Stepsize (years) 1	10	20	100	200	1000
A) Long Term						
1000	.002704	.002698	.002488	.002323	-.000686	-.001907
2000	-	.005273	.005067	-	-.003301	-.003134
3000	-	.007706	.007506	.007308	-.005799	-.005536
4000	-	.009971	.009779	.009568	-.008153	-.007995
5000	-	.012033	.011852	.011632	-.010325	-.010324
B) Intermediate Term						
200	.000552			.000259		
400	.001097			.000743		
600	.001638			.001270		
800	.002174			.001798		
1000	.002704			.002323		

integration would take about 1.5 hours of computer time with the 100 year stepsize and proportionately longer with the smaller step.

Further tests were made using the averaged equations of motion. Since the euqations integrate average elements, the initial elements must be average ones rather than osculating elements. Average elements were computed over a 20 year interval which is nearly the synodic period of Jupiter and Saturn. This should be the longest period significant perturbation on non-resonant orbits in the inner solar system. The short period eccentricity variations are illustrated in Figure 2-3 for the calendar interval 1965 to 1995; these results were computed by integrating forward and backward 15 years from the 1980.0 epoch. The corresponding average elements are:

$$\bar{a} = 0.85993 \text{ AU}$$
$$\bar{e} = 4.34 \times 10^{-4}$$
$$\bar{i} = 1.999°$$

The only significant change between the averaged and osculating elements occurs in eccentricity where the average value is over 40 times the initial (osculating) value, but this is still essentially circular for applications purposes. As will be discussed in more detail later, there are indications that the nominal 0.8600 AU orbit is perhaps affected by a nearby resonance, namely, the 5:4 communsurability with Earth, which is exact at a = 0.861774 AU. To insure that the results were not modified due to proximity to the resonance, the nominal storage orbit was changed to one with a semimajor axis of 0.85 AU. An integration using this new orbit with initial elements $e = 1 \times 10^{-5}$, $i = 2.0°$ yielded mean elements of $\bar{e} = 1.46 \times 10^{-4}$ and $\bar{i} = 2.0003°$; however, even in this orbit, the mean eccentricity is still much larger than in initial osculating value. A better initial orbit for comparison between integrated and averaged equations is one that has initial osculating elements the same order of magnitude as the averaged elements. For semimajor axes around 0.85 AU, the mean eccentricity is typically $(1\text{-}5) \times 10^{-4}$. This value is comparable to

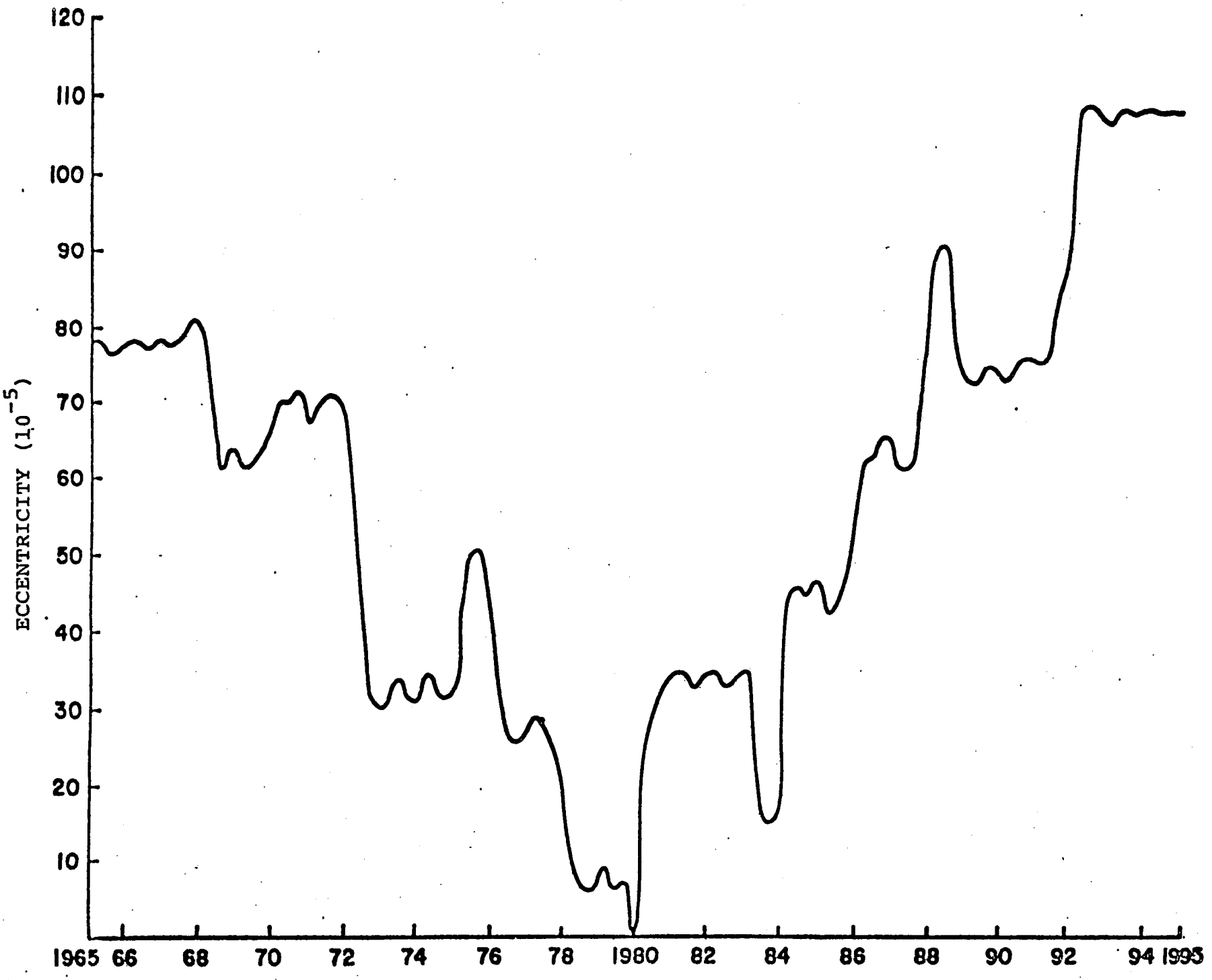

FIGURE 2-3 ECCENTRICITY VARIATION FOR NEARLY CIRCULAR ORBIT AT 0.86 AU.

the expected eccentricity resulting from guidance and execution errors associated with the insertion process which were shown to have a standard deviation of $\sim 4 \times 10^{-4}$ at this heliocentric distance (Friedlander et al. [1]). In light of these considerations, an initial osculating eccentricity of 5×10^{-4} was chosen which resulted in the average elements $\bar{a} = 0.849975$, $\bar{e} = 4.03 \times 10^{-4}$, and $\bar{i} = 1.998$. Integration accuracy tests were performed with the averaged equations using these initial conditions and are summarized in Table 2-3. The comparisons based on this orbit indicate little loss of accuracy in going from stepsizes of 10 years to 100-200 years. In light of these results, a 100 year timestep was used for numerical integration of the averaged equations.

Numerical integration accuracies over longer intervals may be estimated based on analysis by Brouwer [7], who showed that numerical integration errors accumulate proportional to $n^{3/2}$ for the mean anomaly (position variable in the orbit), but for the other elements errors accumulate only as $n^{1/2}$, where n is the number of integration steps. Assuming an error propagation as $n^{1/2}$ for the eccentricity, an eccentricity difference of 1×10^{-4} in 50 years (Table 2-1) would increase to 0.01 in 500,000 years. For circular orbits midway between Venus and Earth, an eccentricity of 0.08 is required before the orbit can theoretically approach a planet. Hence, the integration error is apparently small compared to the eccentricity variations induced by planetary perturbations over this long time interval.

2.3 Analysis

Before commencing the long-term integration test runs, a 1000 year test run was made comparing the analytic averaged equations, integrated averaged equations and the fully integrated equations for the 0.86 AU initial orbit. As seen from Figure 2-4, the analytic and integrated averaged equations have slightly different slopes, but are essentially in good agreement. This is true only over this limited interval. Clearly, if

TABLE 2-3: ECCENTRICITY COMPARISON OF AVERAGED EQUATIONS WITH DIFFERENT STEPSIZES

Initial Orbit: $\bar{a} = .849975$, $\bar{e} = 4.03 \times 10^{-4}$, $\bar{i} = 1.998^{\circ}$

Time After Epoch (years)	Stepsize (years)					
	All Perturbing Planets				V,E,M,J,S Only Perturbing Planets	
	1000	200	100	10	200	10
200	-	.000644	.000644	.000644	.000641	.000641
400	-	.001083	.001083	.001083	.001073	.001073
600	-	.001556	.001556	.001556	.001539	.001539
800	-	.002037	.002037	.002037	.002013	.002012
1000	.000929	.002482	.002482	.002517	.002486	.002486
2000	.002377	.004830	.004830	-	.004800	-
3000	.004758	.007026	.007026	-	.006977	-
4000	.006980	.009061	.009061	-	.008981	-
5000	.009026	.010902	.010902	-	.010794	-

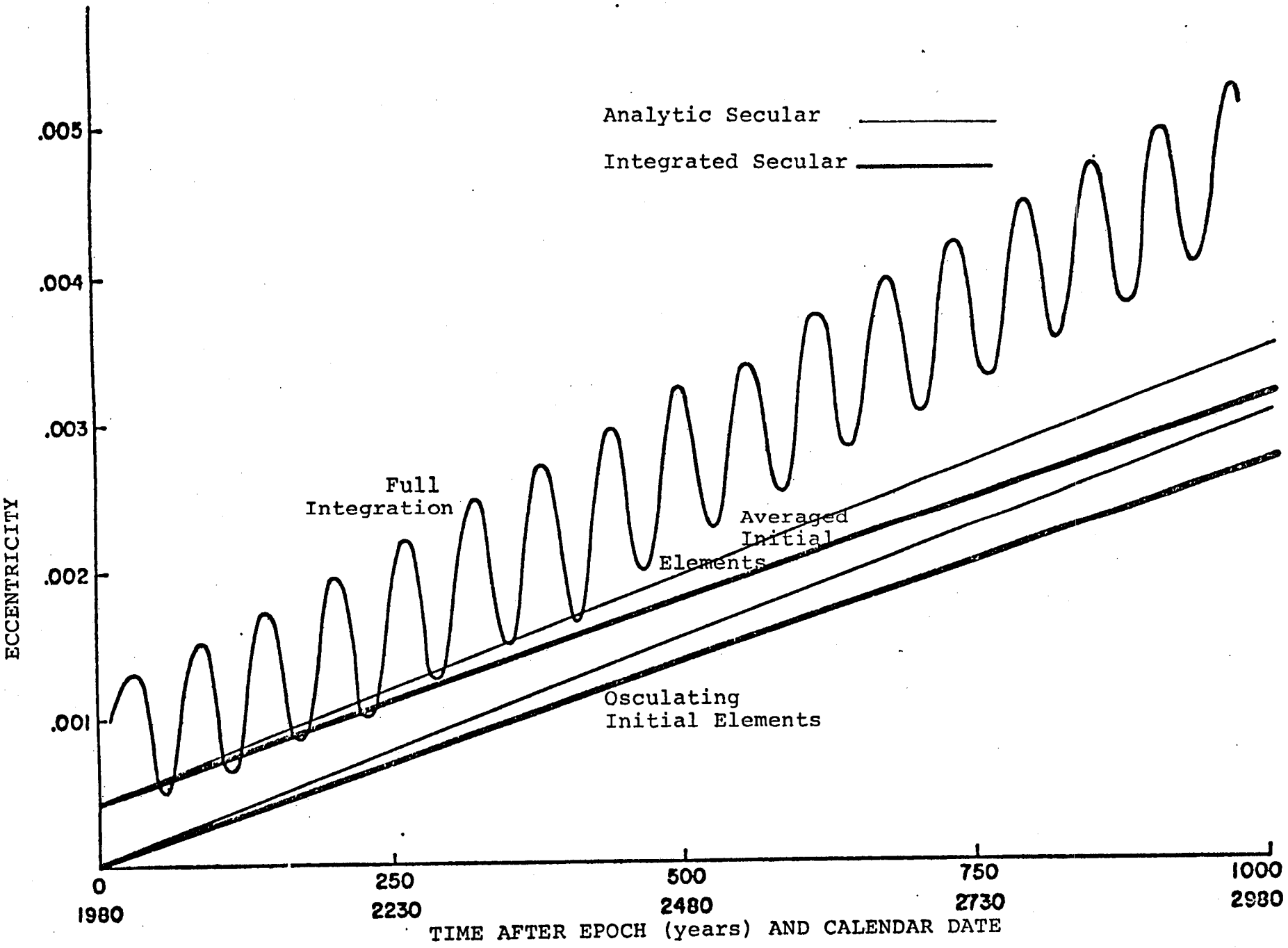

FIGURE 2-4 COMPARISON OF ECCENTRICITY VARIATIONS BASED ON FULL NUMERICAL INTEGRATION, INTEGRATION OF AVERAGED EQUATIONS AND THE ANALYTIC AVERAGED EQUATIONS.

this divergence continued over the full 500,000 years, there could be a major problem. However, as will be shown later, this divergence is due to a slight difference in the period of the secular variation but does not influence the amplitude. The full integration result plots eccentricity averaged over 20 years. For comparison, the results using the averaged equations, but starting with osculating elements, are given.

The divergence of the integrated and averaged results on this short timescale is of some concern and two possible causes were explored: (1) proximity to the 5:4 resonance with Earth, or (2) semimajor axis variations. A 0.85 AU orbit is well away from low order resonances with Earth or Venus. The 1000 year test run was therefore repeated using this orbit (Figure 2-5). The eccentricity variations for the fully integrated orbit are quite different than before, since the large amplitude, 60 year period oscillation has disappeared. The integrated elements now parallel the averaged elements quite well, with only a small divergence in the slopes and a small initial offset. In Figure 2-6, the semimajor axis variation of the 0.86 and 0.85 AU initial orbits are compared and show the much larger amplitude oscillations for the 0.86 AU orbit. These oscillations, which are likely introduced by the nearby resonance, have a mean period of nearly 60 years and probably are responsible for the eccentricity variations with nearly the same period. The more stable 0.85 AU orbit clearly is a better choice for the validation study.

A 500,000 year integration of the 0.85 AU orbit using the averaged equations is compared with analytic secular theory in Figure 2-7. In terms of the heliocentric distances covered and the general behavior of the orbital evolution, the agreement is quite good. The eccentricity amplitudes differ only slightly, and there is no indication that the integrated orbit will approach a planetary orbit in 500,000 years. However, a detailed comparison indicates a small difference in period of some terms in the eccentricity variation. The 25,000 year period variation is slightly longer in the integrated run than in the analytic evaluation; hence, there is an increasing phase difference between the two runs. These differences

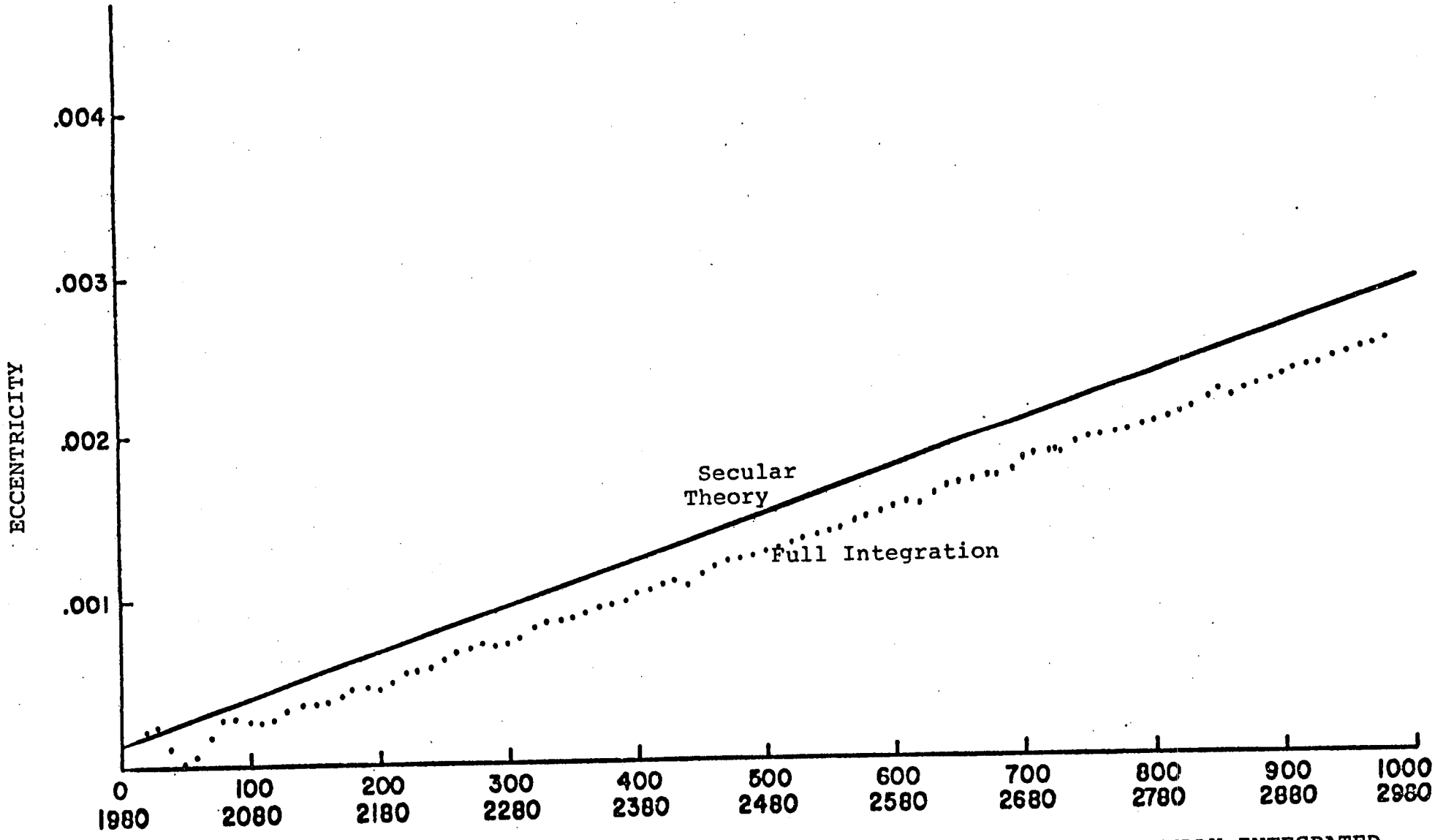

FIGURE 2-5 COMPARISON OF ECCENTRICITY CHANGES FOR 0.85 AU ORBIT. THE FULLY INTEGRATED POINTS ARE AVERAGED OVER 20 YEARS.

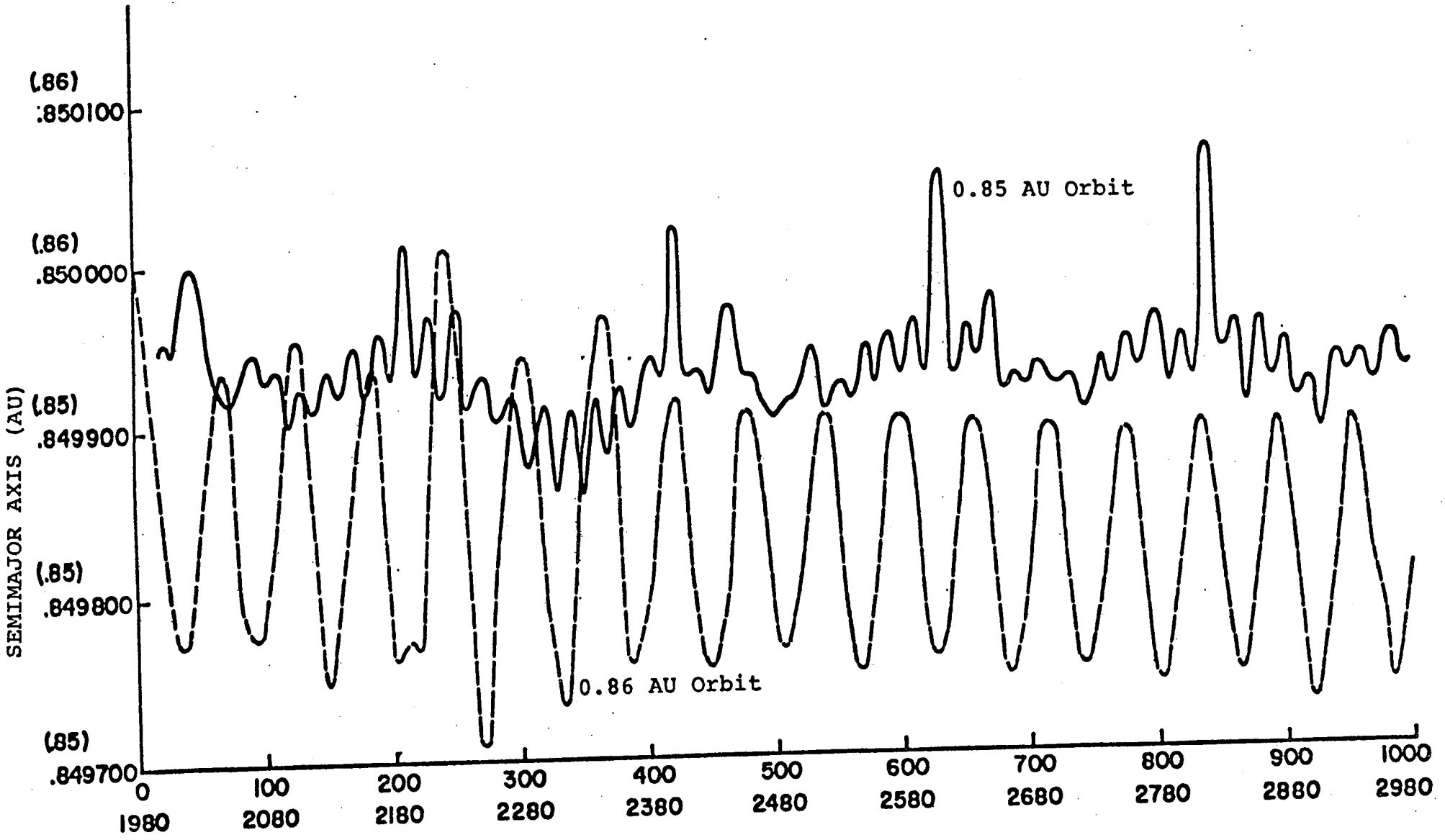

FIGURE 2-6 COMPARISON OF SEMIMAJOR AXIS VARIATIONS FOR 0.85 and 0.86 AU ORBITS

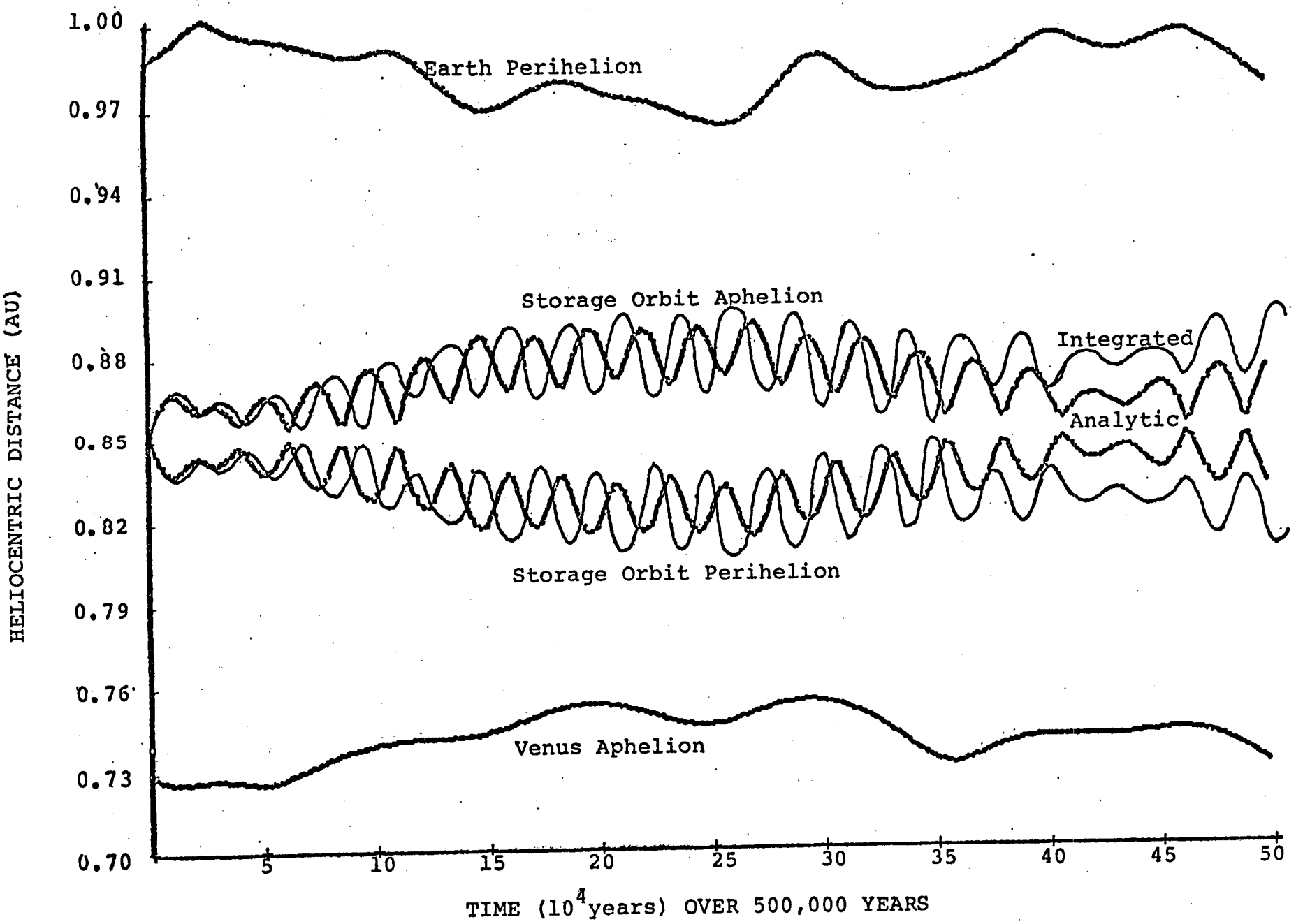

FIGURE 2-7 COMPARISON OF ORBIT VARIATIONS BASED ON ANALYTIC SECULAR THEORY (heavy lines) AND INTEGRATED AVERAGED EQUATIONS (thin lines).

are possibly due to the truncation of higher order terms in formulation of the analytic theory or to an error in one or both solutions. In general, however, there is no significant difference between analytic and integrated averaged equations of motion from the viewpoint of orbital stability.

The most significant test of the averaged equations is to compare their results with those from integration of the full equations of motion. Figure 2-8 compares these results for the 0.85 AU orbit for a 12,000 year interval. Again, the overall agreement is quite good, indicating that secular perturbation theory does accurately describe the long-term evolution of non-resonant orbits, at least on a timescale of 10^4 years.

The period difference that was noted between the full averaged equations and the analytic solution also appears in the fully integrated comparison. The analytic solution shows a slightly shorter period than is indicated by the integrated solution, which is consistent with the trend noted earlier. This difference is of little significance for orbital stability. The important comparison, namely, the range of heliocentric distance covered due to planetary perturbations, shows excellent agreement.

Comparison of integrated averaged euqations and analytic theory for an orbit between Earth and Mars is given in Figure 2-9. The initial orbit is circular at a = 1.19 AU with a 2.0° inclination. The orbital period is 1.298 years which is between the 4:5 and 3:4 resonance with Earth, and based on the ratio of orbital periods with Mars (0.68969) is between the 3:2 and 4:3 Mars commensurability. The exact 3:2 commensurability with Mars (at a = 1.163 AU) is the closest of the two, so the 1.19 AU orbit is well away from any planet resonances. The comparison shown in Figure 2-9 is generally good in that the heliocentric range is about the same between the two runs; however, the period difference still exists in the eccentricity variations. An extended full integration would aid in deciding the source of this discrepancy.

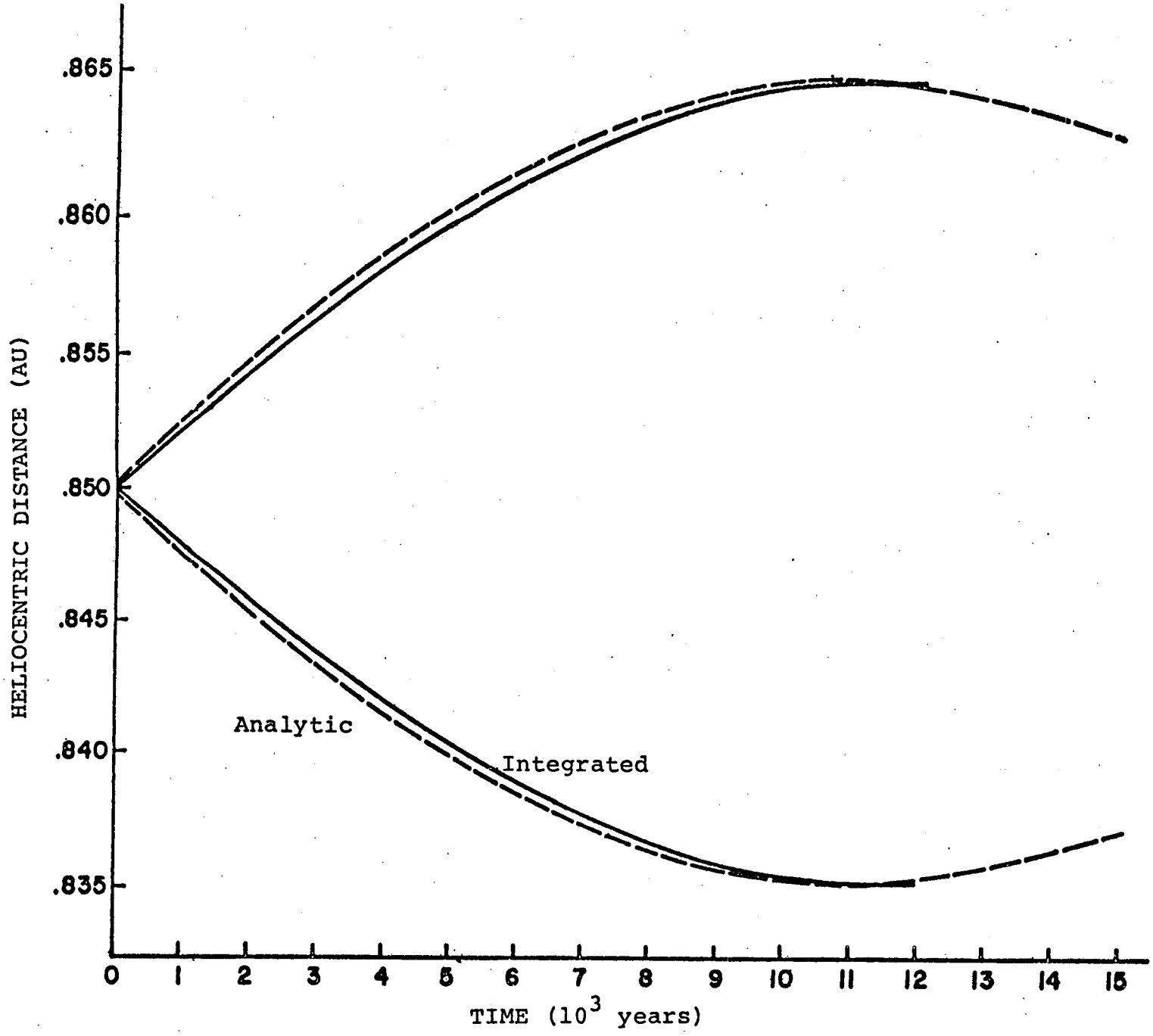

FIGURE 2-8 COMPARISON OF HELIOCENTRIC DISTANCE VARIATIONS BASED ON FULLY INTEGRATED ORBIT (solid line) AND ANALYTIC SECULAR THEORY (dashed line).

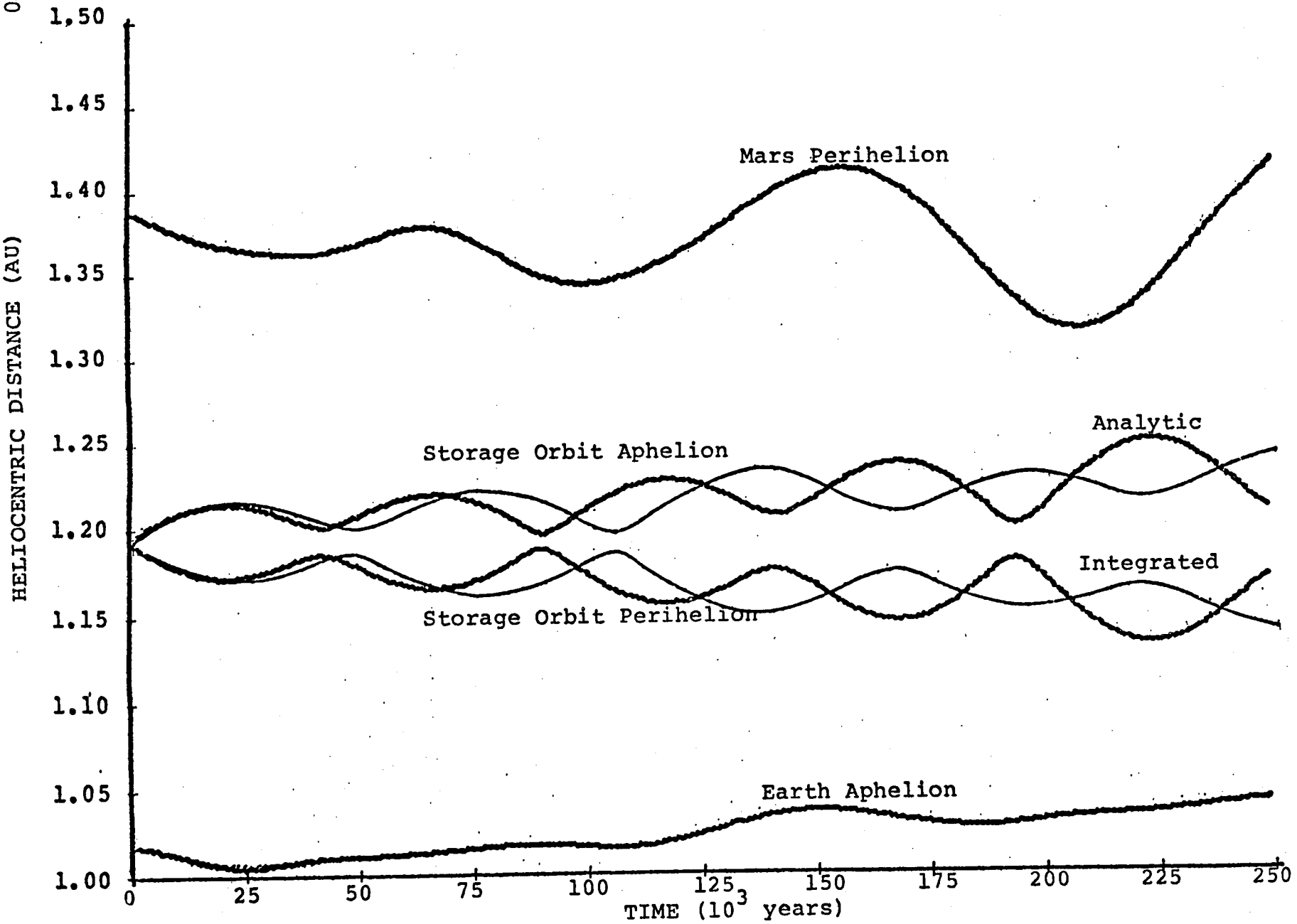

FIGURE 2-9 COMPARISON OF STORAGE ORBIT DISTANCE VARIATIONS BASED ON ANALYTIC SECULAR THEORY (heavy line) AND INTEGRATED AVERAGED EQUATIONS (line line).

2.4 Discussion

The validation of secular perturbation theory in this study shows that the orbital extremes predicted by analytic secular theory are valid for timescales of order 10^4 years and probably for even longer intervals. There is no indication of higher order perturbations resulting from truncation of the full averaged equations in formulating the analytic solution, at least on timescales of order 10^6 years. Certainly from the perspective of waste disposal requirements, storage orbits between Venus and Earth or between Earth and Mars give every indication of meeting the desired stability requirements. The definitive test would, of course, be to do a full numerical integration of the actual equations of motion for 5×10^5 years.

The above conclusion that the solar storage orbits do appear stable should be compared with results of other studies addressing similar questions. One investigation of the stability of the solar system (Birn [8]) claims that there are no stable regions between Venus and Earth, while between Earth and Mars, the stable zone is from 1.16 AU to 1.39 AU. His method for stability analysis is to numerically integrate a four-planet system--Venus, Earth, Mars and Jupiter--for intervals of 700 to 1500 years. Birn employed the device of augmenting the planetary masses to shorten the timescale of dynamical interactions. This method assumes that if there exist secular variations of magnitude m^j in an element (j, an integer, is the order of the perturbation), then increasing the mass of the perturbing body (m) by a factor of f, will increase the magnitude of this term after time t, by a factor of f^j. If an integration of T years is required to detect this secular variation due to m, then only an interval $T/(f^j)$ is required for the augmented mass case. For example, if there are secular terms of order m^3 in the semimajor axis as discovered by Haretu in 1885*, an increase in perturbing mass of 10 would increase the magnitude

*More recent work by Message [9] indicates that this is just the leading term in a truly periodic function and that there are no known truly secular terms in semimajor axis to any order.

of this secular term by 1000. If it takes a 10^6 year integration to detect secular terms using a perturbing mass m, they should be detectable in 1000 years with a perturbing mass of 10m. This method also assumes that other dynamical features of the problem such as the amplitude of periodic terms are not changed by the augmented mass.

Birn found that orbits in the terrestrial planet gaps became unstable on accelerated timescales from 10 to 30 years when the masses of the terrestrial planets were augmented by 100 and that of Jupiter by 10. However, there is no discussion of the behavior of individual orbit elements, particularly a and e, nor of the physical nature of the instability.

Presumably instability is caused by perturbations on the planetesimal orbit (a and/or e) causing it to become a planet-crossing orbit and to be eliminated by impact or ejection. It is well-known that there are no secular changes to a through second order in m but there are first order changes to e (hence the name secular perturbation theory!). Increasing the masses of Earth and Venus by 100 would increase the magnitude of these terms by the same factor (assuming that Venus and Earth perturbations are dominant for an orbit midway between these planets). As was noted earlier and can be seen from Figure 2-1, eccentricities around 0.08 theoretically allow the planetesimal to become planet-crossing, while eccentricities twice as large guarantee that it will be planet-crossing. From Figure 2-5, the 0.85 AU orbit develops an eccentricity of 0.0008 on a timescale of 300 real years and a value of 0.0016 in about 600 years. With a 100-fold increase in the perturbing mass, the eccentricity should be 0.08 to 0.16 within 3 to 6 accelerated years, beyond which time a collision or close planetary encounter becomes a matter of random chance as described in Section 3. These times are reasonably consistent with Birn's range of 10 to 30 accelerated years for instability. However, if the above scenario is the cause of instability, it indicates a flaw in the method for it is well-known that secular perturbation theory gives periodic variations in the eccentricity on long timescales (Figure 2-1). Increasing the initial,

apparently secular change (Figure 2-5) to the point where the orbit becomes planet-crossing changes the dynamical nature of the problem, i.e., the augmented perturbations seem to have introduced the instability. Note also that the first-order scaling would indicate instability on times of 1000 to 3000 years for the actual solar system whereas this study shows stability to 12,000 years for the present-day solar system. If the semimajor axis has secular variations, i.e., if there is a third order secular increase in $\underline{a}$, then orbits should be stable for times of 10^4 to 10^7 years (the fact that planetary masses were changed by different factors makes it somewhat difficult to scale the results). The lower number results if Jupiter perturbations are dominant while the larger one holds if Venus and Earth are the largest perturbers. It should be pointed out, that for the outer planets, Birn argues that for a 100-fold increase in planetary masses, only the present-day semimajor axes of these planets are stable. However, in contrast to this conclusion, Nacozy [10] finds that Saturn would become unstable if the Jupiter-Saturn system mass is increased by 29.25. It is clear that further work is required in this area to understand the physical nature of the alledged instability and the timescale on which it occurs.

In summary, the present study shows by numerical integration that orbits between Venus and Earth are definitely stable on timescales of 10^4 years, while integration of the averaged equations shows that orbits between Venus and Earth or between Earth and Mars are stable for at least 5×10^5 years. No indications of incipient instability were found during the integration runs. Conflicting results regarding stability of orbits between Venus and Earth are attributed to differences in the dynamical models, and it is questioned whether results based on augmenting the masses of perturbing bodies are comparable to those presented in this study.

Section 2 References

2.1 Friedlander, A. L., H. Feingold, D. R. Davis and R. J. Greenberg (1977), "Aborted Space Disposal of Hazardous Material: The Long-Term Risk of Earth Reencounter," SAI Report No. 1-120-676-T8.

2.2 Brouwer, D., and G. M. Clemence (1961), Methods of Celestial Mechanics, Academic Press, New York.

2.3 Brouwer, D. (1951), "Secular Variations of the Orbital Elements of Minor Planets," Astron. J. 56, pp. 9-32.

2.4 Brouwer, D. and J.J.J. Van Woerkam (1950), "The Secular Variations of the Orbital Elements of the Principal Planets," Astron. Papers Amer. Ephemeris 13, Part II, pp. 85-107.

2.5 Cohen, C. J., E. C. Hubbard and C. Oesterwinter (1973), "Planetary Elements for 10,000,000 Years," Celestial Mechanics 7, pp. 438-448.

2.6 Williams, J. G. and G. S. Benson (1971), "Resonances in the Neptune-Pluto System," Astron. J. 76, pp. 167-177.

2.7 Brouwer, D. (1937), "On the Accumulation of Errors in Numerical Integration," A. J. XLVI, p. 149.

2.8 Birn, J. (1973), "On the Stability of the Planetary System," Astron. and Astrophys. 24, pp. 283-293.

2.9 Message, J. (1976), "Formal Expressions for the Motion of N Planets in the Plane with the Secular Variations Included, and an Extension to Poisson's Theorem," in Long-Time Predictions in Dynamics, V. Szebehely and B. D. Tapley, eds. (NATO Adv. Study Ins. Ser.).

2.10 Nacozy, P. (1976), "On the Stability of the Solar System," Astron. J. 81, pp. 787-791.

3. VALIDATION OF EARTH REENTRY RISK

The field of statistical celestial mechanics, developed in the 1950's by the pioneering work of Ernst Öpik, is now recognized as an important contribution to scientific inquiry of solar system evolution and processes. Its principal application has been to studies of asteroid collisions, planet cratering and related cosmogonic processes. The need for a statistical representation of actual events (past or future) derives from the practical limitations of classical celestial mechanics to definitively model orbital evolution over millions of years. This is especially the case when such evolution involves strong gravitational interaction resulting from repeated close planetary encounters. Öpik's analytic theory, based on geometrical reasoning and convincing arguments of averaging, is simple in form and allows rapid evaluation of event statistics.

A nuclear waste payload which fails to achieve its "stable" destination orbit may be considered a stray body in the solar system. Stray bodies in interplanetary space which cross and possibly intersect the orbits of planets define a long-term process of probable orbital change and eventual elimination through the events of planet collision, solar impact or solar system escape. The problem of quantifying the probabilistic fate of a failed payload is identical in all respects to the general problem of statistical celestial mechanics. Öpik's theory was utilized in the development of the PEPA computer program from which previous study results were generated [1]. These results are thought to represent "statistical truth" to within a close order-of-magnitude, i.e., a factor of 2 to 5. It is the verification of this presumption which is the subject of this section of the report.

3.1 Monte Carlo Simulation of Planetary Encounters

Since Öpik's formulae are based on averaging approximations to real world orbital perturbations, certain limitations of the analytical approach arise when dealing with complex problems. The main difficulty is related to the following two factors: (1) the dispersion in relative encounter

velocity magnitude caused by successive close encounters with a real planet moving in a precessing, elliptical orbit rather than a fixed circular orbit; and (2) the dispersion caused by multiple close encounters with more than one planet resulting in a "playing ball with the particle" effect. This dispersion or so-called acceleration of encounter speed is not accounted for in the basic theory. Although Öpik in his later work recognized and explained the acceleration effect, after it was discovered empirically, it is difficult to ammend the formulae in a simple, straightforward way to properly account for this effect. In contrast, the problem is readily treated by numerical simulation using Monte Carlo statistical methods.

Other science researchers, most notably Arnold [2,3] and Wetherill [4,5], have extended the treatment of statistical celestial mechanics by adopting the numerical approach and we follow their lead here. The result is a semianalytic method in that Öpik's equations, which give the probability of close planetary encounter, are used in an iterative manner to drive a Monte Carlo generator of orbital evolution and collisional statistics. The method proceeds as follows:

1. Input initial orbit elements (a,e,i) at time T.
2. Identify all planets whose orbits may be crossed by the stray body.
3. Using Öpik's equations, calculate the probability of close approach (within K collision radii) to each planet. A typical choice is K = 5.
4. Combine these probabilities to calculate a mean time (τ) between encounters.
5. Choose the next planet to be encountered, at random, weighted according to the relative encounter probabilities.
6. Choose a time interval ΔT to the next encounter, at random, from an exponential distribution $e^{-\Delta T}/\tau$. Record the running time $T \rightarrow T + \Delta T$.

7. Choose a random location on the encountered planet's orbit within the allowable region of orbit crossing.

8. Choose a random point on a target disk of K collision radii centered on the chosen planet. The stray body is assumed to move on a hyperbolic relative trajectory passing through this point. The region (K/2,K) is weighted more heavily than the interior region (0,K/2) so as to account for those passages outside of K radii which may occur but are ignored for reasons of computational efficiency.

9. If collision does not occur, calculate the change in orbit elements produced by the close gravitational encounter.

10. Use the new orbit elements to reinitialize Step (1).

11. Continue this procedure until some event terminates the evolution process (planet collision, solar impact or solar system escape).

12. Upon termination of a given Monte Carlo pass, recycle to the original orbit state and repeat the entire random experiment. Statistics are accumulated over a large number (several hundred) of passes.

This methodology may be recognized as a statistical analog of a multi-revolution numerical integrator. It also involves approximations to reality but at a higher level of accuracy compared to the strictly analytic, closed-form theory. Also, the results could be sensitive to the sequence of random number generation and the total number of Monte Carlo passes. As in any finite sampling experiment, care must be taken to generate a sufficient number of cases so as to have reasonable confidence in the statistical data. In practice, this implies the usual trade-off between statistical variability and computational cost.

The Monte Carlo simulation outlined above was programmed as a modification to the existing computer program PEPA. The new subroutine may be selected upon user option in place of the analytic formulae for the computation of event probabilities conditional upon the specified initial orbit. A variety of test cases were run with reference to data published

by Wetherill to assure that the program worked properly. Application was then made to the waste disposal problem as described in the remainder of this section.

3.2 Comparison of Conditional Probability Results

Before presenting example results, it will be helpful to review the basic definitions of "conditional probability" and "total probability." Conditional probability of an event E refers to the likelihood that the event will occur within a specified (long) time interval T given that the payload is left in an unstable orbit having initial conditions (a,e,i;t) resulting from a deployment system failure at time t. The point of failure occurs somewhere in the (short) time interval $(0,t_f)$ comprising the nominal deployment sequence. Total probability then refers to the likelihood of this same event as obtained by integrating the entire spectrum of conditional probability over the time distribution of deployment system failures. Let R(t) denote the reliability function for the deployment system. Total probability may be computed from the integral expression

$$P_E(T) = \int_0^{t_f} P_E(T|t) \left| \frac{dR(t)}{dt} \right| dt$$

where $P_E(T|t)$ is the conditional probability of the event. Staged propulsion sequences and startup reliability are readily accommodated in the definition of R(t). The PEPA program uses Simpson's Rule integration to evaluate total probability.

In assessing the validity of previously obtained analytic results, it is the conditional probability $P_E(T|t)$ that is of chief concern and, in particular, the event of Earth collision or reentry. In other words, does Monte Carlo simulation give essentially the same results for $P_E(T|t)$ as predicted by Öpik's theory, or is there a significant discrepancy? We have reason to expect some difference because of the encounter speed

dispersion effect that was mentioned earlier. This dispersion is particularly important when the initial value is small, e.g., less than 0.1 of Earth mean orbital speed. This is in fact the situation of interest for an Earth-crossing orbit having dimensions close to that of the Earth's orbit and inclined to the Earth's orbit by a small angle.

Consider an initial orbit of size 0.86 × 1.0 AU with a 2° inclination to the ecliptic plane. The Earth is the only planet that is crossed initially. However, the first velocity dispersion factor opens an efficient loophole to the eventual occurrence of Venus crossing. When that happens the second dispersion factor comes into play with eventual crossing of Mars, then Jupiter. Once Jupiter is crossed its enormous gravitational field, on close encounter, can easily cause the object to be ejected from the solar system. Hence, we are dealing with a dynamic process that can lead to many different kinds of elimination events even though Earth collision may be the only event that can occur initially. This process of velocity dispersion or acceleration takes time to build up through numerous close but non-colliding encounters with Earth. The key question then from a probabilistic point-of-view is whether the time constant of this dynamic process is short or long compared to the time interval (e.g., $T \leq 10^6$ years) of concern for waste disposal risk. If the time constant is long, then we can expect fairly close agreement with the analytic prediction.

A computer printout of results is shown in Table 3-1 for the conditional orbit resulting from failure of the circularizing burn at 0.86 AU. Öpik's theory predicts a mean lifetime against Earth collision of $\tau = 0.52 \times 10^6$ years with the probability being exponentially distributed as $1 - \exp(-T/\tau)$. The Monte Carlo simulation shows widely different results for elimination lifetime. Earth collision remains the most likely event of elimination, but only 55.8% of all cases result in this disposition. Furthermore, the mean time of Earth collision is 16.4×10^6 years which is substantially longer than the analytic value. Venus collision is the next most likely event at 29.2% followed by solar system ejection

Table 3-1

MONTE CARLO SIMULATION OF STRAY BODY LIFETIME

Initial Orbit Conditions: $a_0 = 0.93$ AU, $e_0 = 0.075$ } 0.86 × 1.0 AU
$i_0 = 2°$
$U_0 = 0.062$ (at Earth)

MONTE-CARLO STATISTICAL SUMMARY

NUMBER OF CASES = 500
MEAN LIFETIME = .373+08 YEARS

EVENT	NUMBER	FREQUENCY	MEAN TIME	MEAN U
COLLISION WITH PLANET				
MERCUR	8	.0160	.448+08	.490
VENUS	146	.2920	.241+08	.264
EARTH	279	.5580	.164+08	.172
MARS	10	.0200	.534+09	.352
JUPITE	4	.0080	.555+08	.619
SATURN	0	.0000	.000	.750
URANUS	0	.0000	.000	.000
NEPTUN	0	.0000	.000	.000
PLUTO	0	.0000	.000	.000
SOLAR IMPACT	0	.0000	.000	
SOLAR SYSTEM EJECTION	53	.1060	.872+08	

MEAN ELEMENTS AT ELIMINATION
A= 3.020 E= .267 I= 7.79

(due to Jupiter and Saturn crossings) at 10.6%. The combined mean lifetime against all possible events of elimination is 37.3×10^6 years. Note that the mean value of Earth encounter speed at the time of collision is 0.172 EMOS which indicates the substantial dispersion from the initial value of 0.062 EMOS.

The first conclusion we may draw from this test is that the dispersion effect, not accounted for by the analytic theory, acts to increase the lifetime for this particular initial orbit. Although this result is certainly desirable in that the probability of Earth collision is decreased, the real significance depends on the time interval of interest. The time profile is shown in Figure 3-1 which compares the Monte Carlo statistics with the analytic value of Earth collision probability. The agreement is fairly close for $T < 10^5$ years. The largest difference, at $T \sim 10^6$ years, is only a factor of 3.8. Hence, the statement that analytic theory should predict the Earth collision probability to within a close order-of-magnitude appears to be correct.

An analysis of Monte Carlo sampling variations is presented in Table 3-2 for the conditional orbit 0.86 × 1.0 AU. Earth collision probability values are listed for a range of time intervals showing statistical data variations over five sampling cases each for 100 and 500 samples per case. As expected, the data accuracy (standard deviation) improves with larger sample size and longer time interval. With 100 samples, the standard deviations about the mean value are 44.8%, 25.7% and 13.6%, respectively, for time intervals of 10^5, 10^6 and 10^7 years. Corresponding results for 500 samples are 13.3%, 5.1% and 4.7%. These variations are sufficiently small to place reasonable confidence in the results of a finite sampling experiment, i.e., as it pertains to characteristic differences between the analytic and numerical methods.

A comparison of the two methods was also made for a very different initial orbit, namely, one with perihelion distance near Earth and aphelion distance near Jupiter. In this case the dominant event of elimination is

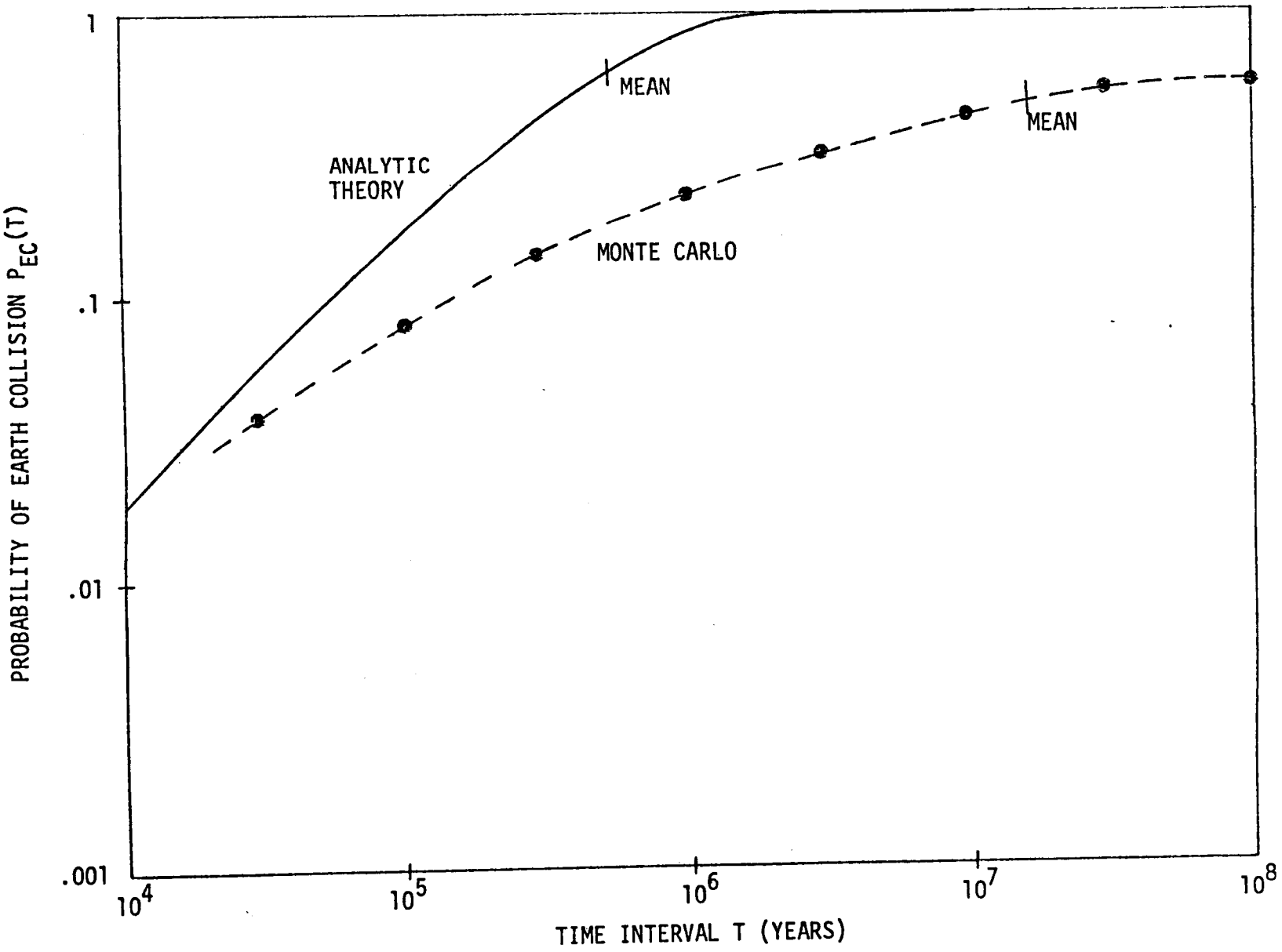

Fig. 3-1 CONDITIONAL PROBABILITY OF EARTH COLLISION (0.86 x 1.0 AU, $i = 2^o$)

Table 3-2

MONTE CARLO SAMPLING VARIATIONS

Conditional Initial Orbit = 0.86 x 1.0 AU, i = 2^{o}
Probability of Earth Collision Within Stated Time Interval

	Case	$T = 10^5$ yrs	$T = 10^6$ yrs	$T = 10^7$ yrs	$T = \infty$
• 100 SAMPLES/CASE	1	0.040	0.120	0.310	0.480
	2	0.060	0.210	0.470	0.590
	3	0.120	0.250	0.440	0.600
	4	0.050	0.170	0.450	0.550
	5	0.050	0.260	0.450	0.600
	Mean	0.064	0.202	0.424	0.564
	S.D.	0.029 (44.8%)	0.052 (25.7%)	0.058 (13.6%)	0.046 (8.1%)
• 500 SAMPLES/CASE	1	0.064	0.200	0.420	0.564
	2	0.058	0.210	0.420	0.552
	3	0.046	0.180	0.390	0.558
	4	0.068	0.190	0.380	0.536
	5	0.054	0.200	0.430	0.584
	Mean	0.058	0.196	0.408	0.559
	S.D.	0.008 (13.3%)	0.010 (5.1%)	0.019 (4.7%)	0.016 (2.9%)

ejection out of the solar system due mainly to Jupiter encounters. The probability of Jupiter collision is about an order of magnitude less than ejection but much greater than any other planet collision event. Results are shown in Figure 3-2 where the probability of occurrence of the two dominant events are plotted as a function of time over the interval 10^5 to 5×10^7 years. Monte Carlo and analytic results are in very good agreement for ejection and somewhat less so for Jupiter collision--but still within a factor of 3. Even though Earth's orbit is crossed by this initial orbit the probability of Earth collision is relatively low. Analytic theory predicts a value of 10^{-4} for $T = 5 \times 10^6$ years. In 1500 Monte Carlo samples only one Earth collision event was observed. Although a much larger sample size would be needed in this case for an accurate comparison with analytic theory, the limited data obtained does not indicate any major discrepancy.

3.3 Comparison of Total Probability Results

The following three waste disposal mission examples were selected for purposes of risk verification:

1. Solar storage orbit, 0.86 AU, 2° inclination
2. Solar storage orbit, 1.19 AU, 2° inclination
3. Solar system escape, 0° inclination.

The propulsion system assumed for the two cases of solar orbit deployment is a reusable OTV at injection and a kick stage for circularization at the nominal heliocentric distance (see Section 4). Although the solar system escape mission is not currently considered a baseline option, it is included here for completeness since it had been exampled previously [1]. A three-stage (large solids) propulsion system is assumed for this case.

The propulsion system failure model, taken to be identical for each stage, includes a startup component (reliability R_{ST}) and an operational component (end-point reliability R_{EP}). For purposes of the risk verification analysis we will simply assume that $R_{ST} = R_{EP} = 0.99$. The effect of the system reliability level will be described parametrically later in Section 3.4.

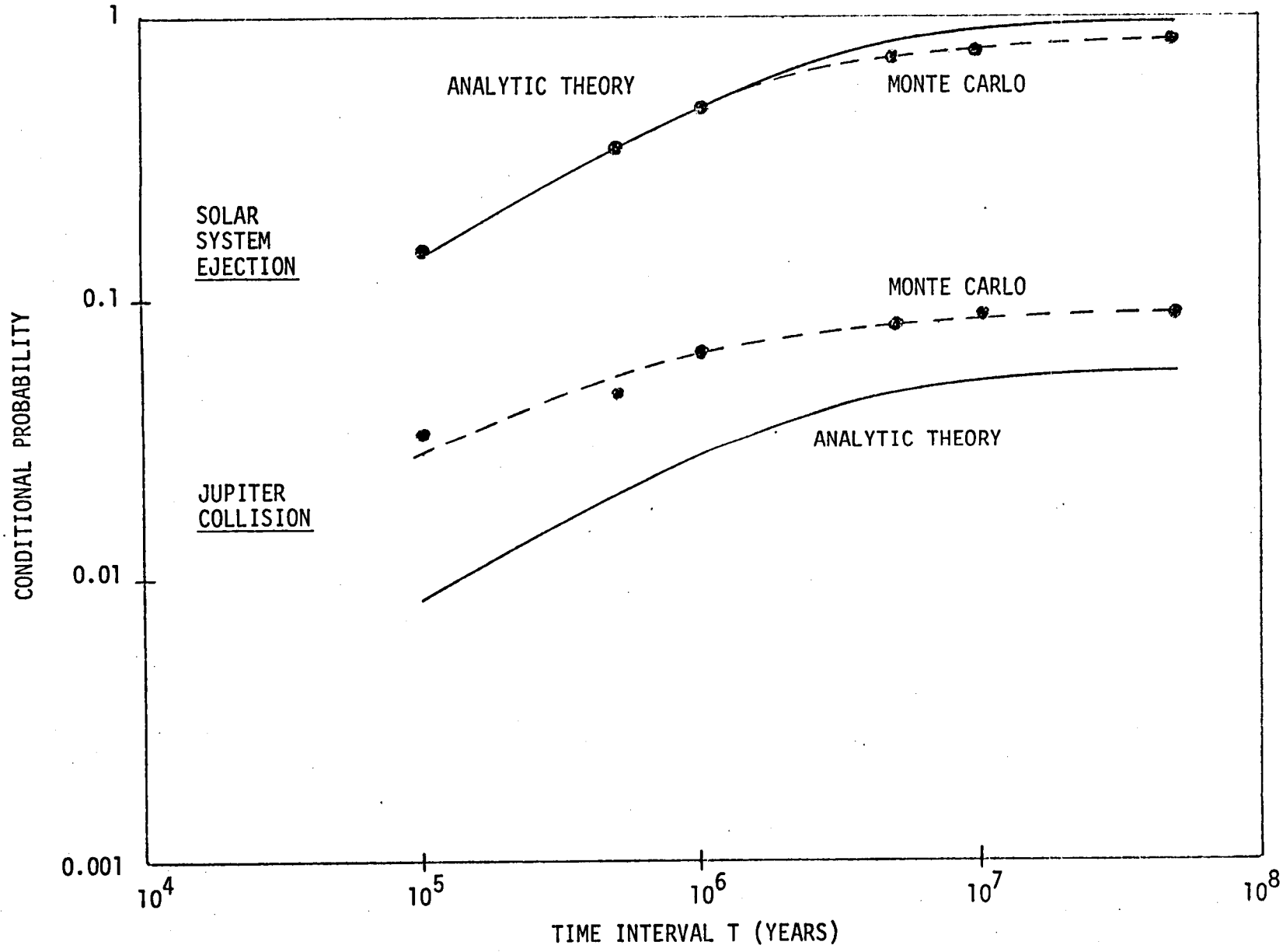

Fig. 3-2 CONDITIONAL PROBABILITY OF EJECTION AND JUPITER COLLISION (0.998 x 5.311 AU, $i = 0^o$)

We examine first the case of the 0.86 AU solar orbit destination. The range of conditional failure orbits encompasses perihelion distances from 1.0 to 0.86 AU and aphelion distances from 1.0 to 0.86 AU. Total or integrated probability data are presented in Table 3-3 which compares analytic theory and Monte Carlo computer printouts. Earth collision is the only event of elimination predicted by analytic theory with probability varying from 2.7×10^{-3} for $T = 10^5$ years to an asymptotic upper limit of 1.3×10^{-2}. Monte Carlo results verify that Earth collision is the dominant event for shorter time intervals, but that other events, notably Venus collision and solar system ejection, become increasingly as likely as time grows. Figure 3-3 compares the probability versus time distribution for Earth collision--the event of primary interest to disposal risk assessment. Monte Carlo results show a probability variation of 6.4×10^{-4} to 5.7×10^{-3} over the time interval 10^5 to 10^7 years. This represents a reduced risk relative to analytic theory prediction by a factor of 5 or less. These results are consistent with the conditional probability comparison discussed earlier and with the accuracy bounds expected of the analytic theory.

Similar data are presented in Tables 3-4 and 3-5 and Figures 3-4 and 3-5, respectively, for the 1.19 AU solar orbit and the solar system escape missions. The probability characteristic and comparison with analytic theory of the 1.19 AU case is nearly the same as for the 0.86 AU disposal destination. Monte Carlo results indicate a reduced risk of Earth collision by a factor of 5. For the solar system escape destination, a much closer agreement is found between analytic and numerical methods. Earth collision probability predicted by analytic theory varies from 2.5×10^{-4} to 7.5×10^{-3} over the time interval 10^5 to 10^7 years. Monte Carlo results are 80% higher at $T = 10^5$ years, approximately the same at $T = 10^6$ years, and 40% lower at $T = 10^7$ years.

3.4 Risk Reduction with Rescue Mission Capability

It seems appropriate to revise the waste disposal risk profiles based on the new data obtained from the Monte Carlo analysis. We shall examine the parametric effects of deployment system reliability and risk reduction through retrieval of failed payloads. With reference to the 0.86 AU solar orbit mission, we have found that the probability of Earth collision is $\sim 2 \times 10^{-3}$ over a time interval of 10^6 years. This means in effect that one payload in 500 launches can be expected to return and reenter Earth's atmosphere sometime within 10^6 years after launch. Let us suppose for the sake of argument that a decision maker is risk-adverse and therefore considers this level of risk to be too high. What means are available to reduce the risk? Improving reliability is the most direct way since deployment system failures are responsible for the problem in the first place. System reliability enhancement by design or redundancy is certainly possible, but there is some practical limitation to this approach beyond which it is no longer technically or economically feasible. We have already assumed a nominal reliability level of 99%. Increasing this to 99.9% will only effect a ten-fold reduction in risk. It seems clear that a different approach is needed to obtain substantial improvement--say to a probability level of 10^{-6} or better. Payload retrieval or rescue capability can provide this assurance.

Retrieval is defined here as the ability to send another propulsion system to rendezvous with the failed payload in solar orbit and to place it into the desired stable orbit. Once this capability exists we may as well adopt a policy of redundancy on a mission level. That is, if the first rescue mission fails we launch a second mission, if the second fails we launch a third, etc. Therefore, assume a standby, multiple rescue capability, each having an equal probability of success or reliability R. The term "standby" does not necessarily imply an on-the-pad readiness since the rescue missions may be carried out over a period of several years. The chance of reentry during this early time period is essentially zero.

Table 3-3

TOTAL PROBABILITY DISTRIBUTION COMPARISON FOR SOLAR ORBIT DISPOSAL (a = 0.86 AU, i = 2^0)

A) ANALYTIC THEORY

HIGH-THRUST STAGE RELIABILITY = .9900 .9900
STAGE START RELIABILITY = .9900 .9900
EVENT PROBABILITIES

FOR TIME INTERVAL =	.10+06	.25+06	.50+06	.10+07	.25+07	.50+07
COLLISION WITH PLANET						
MERCUR	.00	.00	.00	.00	.00	.00
VENUS	.00	.00	.00	.00	.00	.00
EARTH	.27-02	.56-02	.88-02	.12-01	.13-01	.13-01
MARS	.00	.00	.00	.00	.00	.00
JUPITE	.00	.00	.00	.00	.00	.00
SATURN	.00	.00	.00	.00	.00	.00
URANUS	.00	.00	.00	.00	.00	.00
NEPTUN	.00	.00	.00	.00	.00	.00
PLUTO	.00	.00	.00	.00	.00	.00
SOLAR IMPACT	.00	.00	.00	.00	.00	.00
SOLAR SYSTEM EJECTION	.00	.00	.00	.00	.00	.00

B) MONTE CARLO

HIGH-THRUST STAGE RELIABILITY = .9900 .9900
STAGE START RELIABILITY = .9900 .9900
EVENT PROBABILITIES

FOR TIME INTERVAL =	.10+06	.25+06	.50+06	.10+07	.10+08	.10+09
COLLISION WITH PLANET						
MERCUR	.00	.00	.00	.00	.20-05	.40-04
VENUS	.50-05	.90-05	.14-03	.31-03	.19-02	.40-02
EARTH	.64-03	.11-02	.15-02	.22-02	.57-02	.69-02
MARS	.00	.00	.00	.00	.20-05	.42-03
JUPITE	.00	.00	.00	.00	.00	.45-04
SATURN	.00	.00	.00	.00	.00	.20-05
URANUS	.00	.00	.00	.00	.00	.00
NEPTUN	.00	.00	.00	.00	.00	.00
PLUTO	.00	.00	.00	.00	.00	.00
SOLAR IMPACT	.00	.00	.00	.00	.00	.00
SOLAR SYSTEM EJECTION	.00	.00	.00	.00	.36-03	.73-02

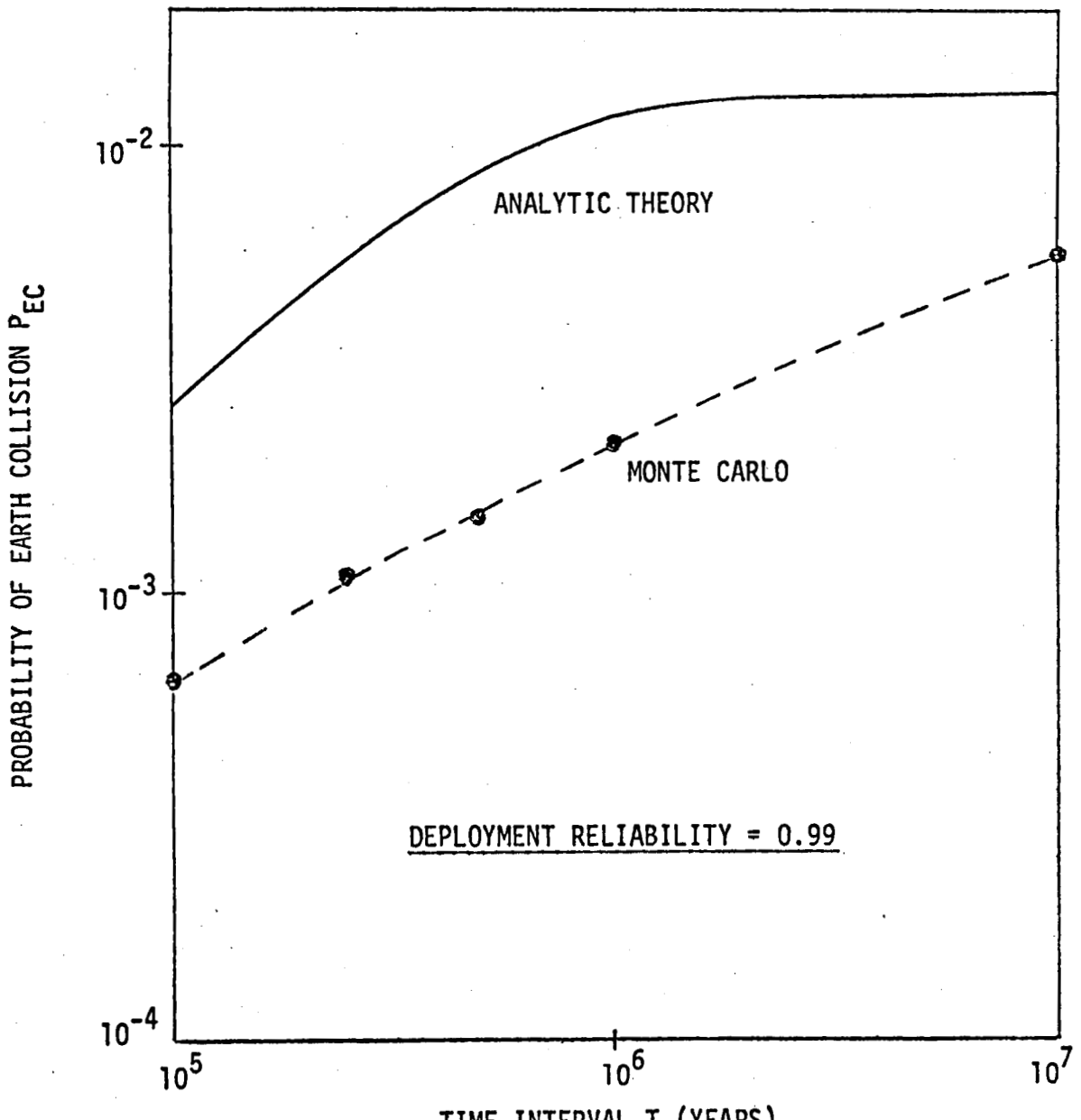

Fig. 3-3 COMPARISON OF ANALYTIC AND MONTE CARLO PREDICTION OF EARTH REENTRY RISK FOR SOLAR ORBIT MISSION (r = 0.86 AU, i = 2^o)

Table 3-4

TOTAL PROBABILITY DISTRIBUTION COMPARISON FOR SOLAR ORBIT DISPOSAL (a = 1.19 AU, i = 2^{o})

A) ANALYTIC THEORY

HIGH-THRUST STAGE RELIABILITY =	.9900	.9900				
STAGE START RELIABILITY =	.9900	.9900				
EVENT PROBABILITIES						
FOR TIME INTERVAL =	.10+06	.25+06	.50+06	.10+07	.25+07	.50+07
COLLISION WITH PLANET						
MERCUR	.00	.00	.00	.00	.00	.00
VENUS	.00	.00	.00	.00	.00	.00
EARTH	.18-02	.40-02	.67-02	.10-01	.13-01	.13-01
MARS	.00	.00	.00	.00	.00	.00
JUPITE	.00	.00	.00	.00	.00	.00
SATURN	.00	.00	.00	.00	.00	.00
URANUS	.00	.00	.00	.00	.00	.00
NEPTUN	.00	.00	.00	.00	.00	.00
PLUTO	.00	.00	.00	.00	.00	.00
SOLAR IMPACT	.00	.00	.00	.00	.00	.00
SOLAR SYSTEM EJECTION	.00	.00	.00	.00	.00	.00

B) MONTE CARLO

HIGH-THRUST STAGE RELIABILITY =	.9900	.9900				
STAGE START RELIABILITY =	.9900	.9900				
EVENT PROBABILITIES						
FOR TIME INTERVAL =	.10+06	.25+06	.50+06	.10+07	.25+07	.50+07
COLLISION WITH PLANET						
MERCUR	.00	.00	.00	.00	.00	.00
VENUS	.50-05	.50-05	.29-04	.26-03	.67-03	.16-02
EARTH	.40-03	.87-03	.14-02	.21-02	.35-02	.47-02
MARS	.00	.00	.00	.20-05	.20-05	.15-04
JUPITE	.00	.00	.00	.00	.00	.00
SATURN	.00	.00	.00	.00	.00	.00
URANUS	.00	.00	.00	.00	.00	.00
NEPTUN	.00	.00	.00	.00	.00	.00
PLUTO	.00	.00	.00	.00	.00	.00
SOLAR IMPACT	.00	.00	.00	.00	.00	.00
SOLAR SYSTEM EJECTION	.00	.00	.00	.00	.00	.00

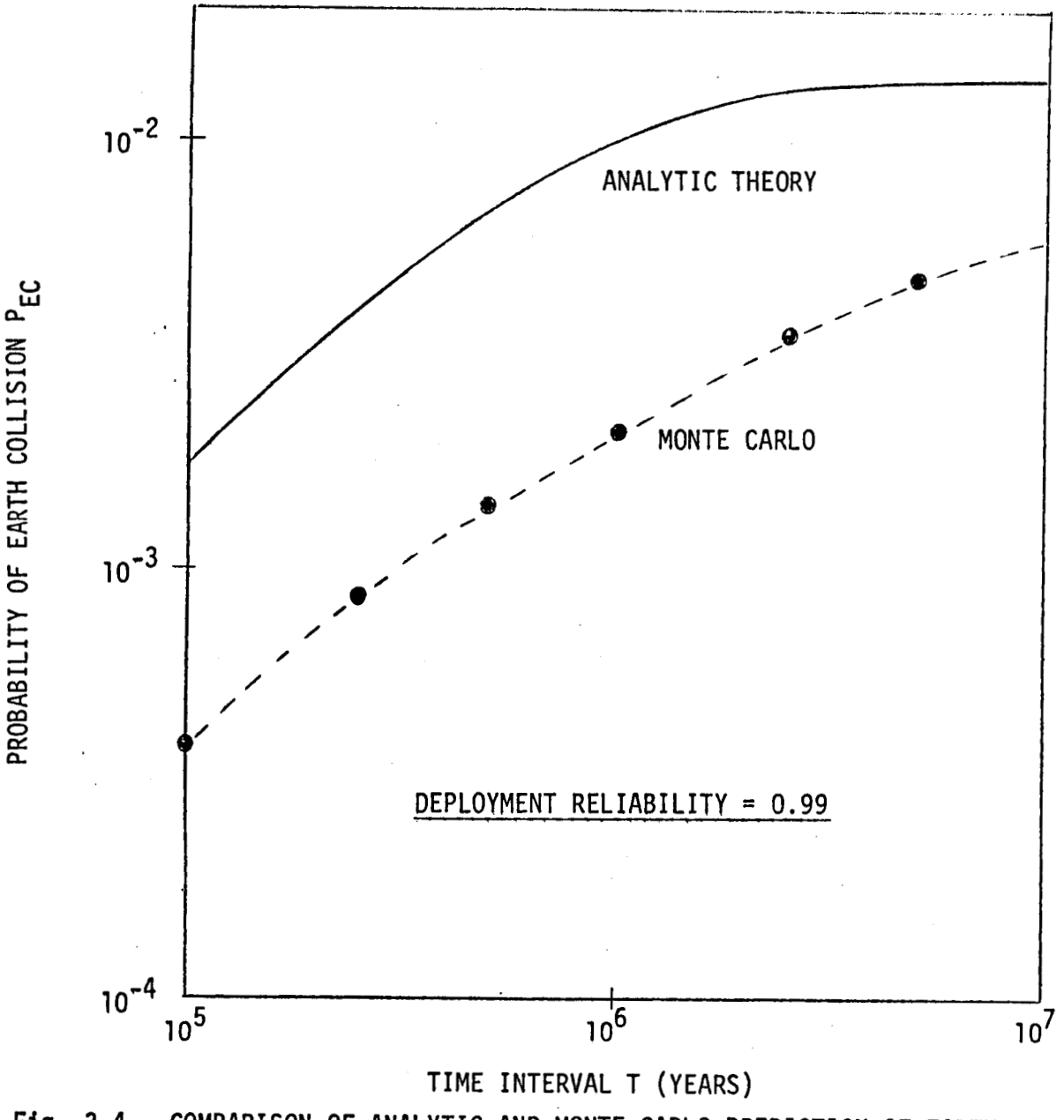

Fig. 3-4 COMPARISON OF ANALYTIC AND MONTE CARLO PREDICTION OF EARTH REENTRY RISK FOR SOLAR ORBIT MISSION (r = 1.19 AU, i = 2°)

Table 3-5

TOTAL PROBABILITY DISTRIBUTION COMPARISON FOR SOLAR SYSTEM ESCAPE DISPOSAL ($i = 0^0$)

A) ANALYTIC THEORY

HIGH-THRUST STAGE RELIABILITY = .9700 .9700 .9700

STAGE START RELIABILITY = .9700 .9700 .9700

EVENT PROBABILITIES FOR TIME INTERVAL =	.10+06	.25+06	.50+06	.10+07	.25+07	.50+07
COLLISION WITH PLANET						
MERCUR	.20-07	.93-07	.25-06	.50-06	.78-06	.11-05
VENUS	.14-04	.76-04	.25-03	.70-03	.20-02	.35-02
EARTH	.71-03	.16-02	.28-02	.47-02	.91-02	.15-01
MARS	.48-05	.11-04	.22-04	.41-04	.87-04	.15-03
JUPITE	.45-04	.77-04	.11-03	.15-03	.21-03	.25-03
SATURN	.28-05	.44-05	.58-05	.77-05	.11-04	.13-04
URANUS	.24-07	.52-07	.84-07	.12-06	.16-06	.19-06
NEPTUN	.50-09	.15-08	.33-08	.69-08	.16-07	.29-07
PLUTO	.42-12	.12-11	.27-11	.55-11	.13-10	.24-10
SOLAR IMPACT	.45-05	.11-04	.21-04	.35-04	.54-04	.68-04
SOLAR SYSTEM EJECTION	.12-02	.20-02	.29-02	.39-02	.54-02	.65-02

B) MONTE CARLO

HIGH-THRUST STAGE RELIABILITY = .9700 .9700 .9700

STAGE START RELIABILITY = .9700 .9700 .9700

EVENT PROBABILITIES FOR TIME INTERVAL =	.10+06	.25+06	.50+06	.10+07	.25+07	.50+07
COLLISION WITH PLANET						
MERCUR	.00	.00	.00	.00	.00	.00
VENUS	.00	.00	.59-04	.19-03	.63-03	.29-02
EARTH	.13-02	.19-02	.35-02	.46-02	.76-02	.12-01
MARS	.00	.49-04	.83-04	.83-04	.38-03	.40-03
JUPITE	.11-03	.11-03	.11-03	.16-03	.29-03	.38-03
SATURN	.16-04	.16-04	.16-04	.16-04	.48-04	.48-04
URANUS	.16-04	.16-04	.16-04	.16-04	.16-04	.16-04
NEPTUN	.00	.00	.00	.00	.00	.00
PLUTO	.00	.00	.00	.00	.00	.00
SOLAR IMPACT	.00	.00	.16-04	.16-04	.16-04	.16-04
SOLAR SYSTEM EJECTION	.54-02	.78-02	.11-01	.14-01	.18-01	.22-01

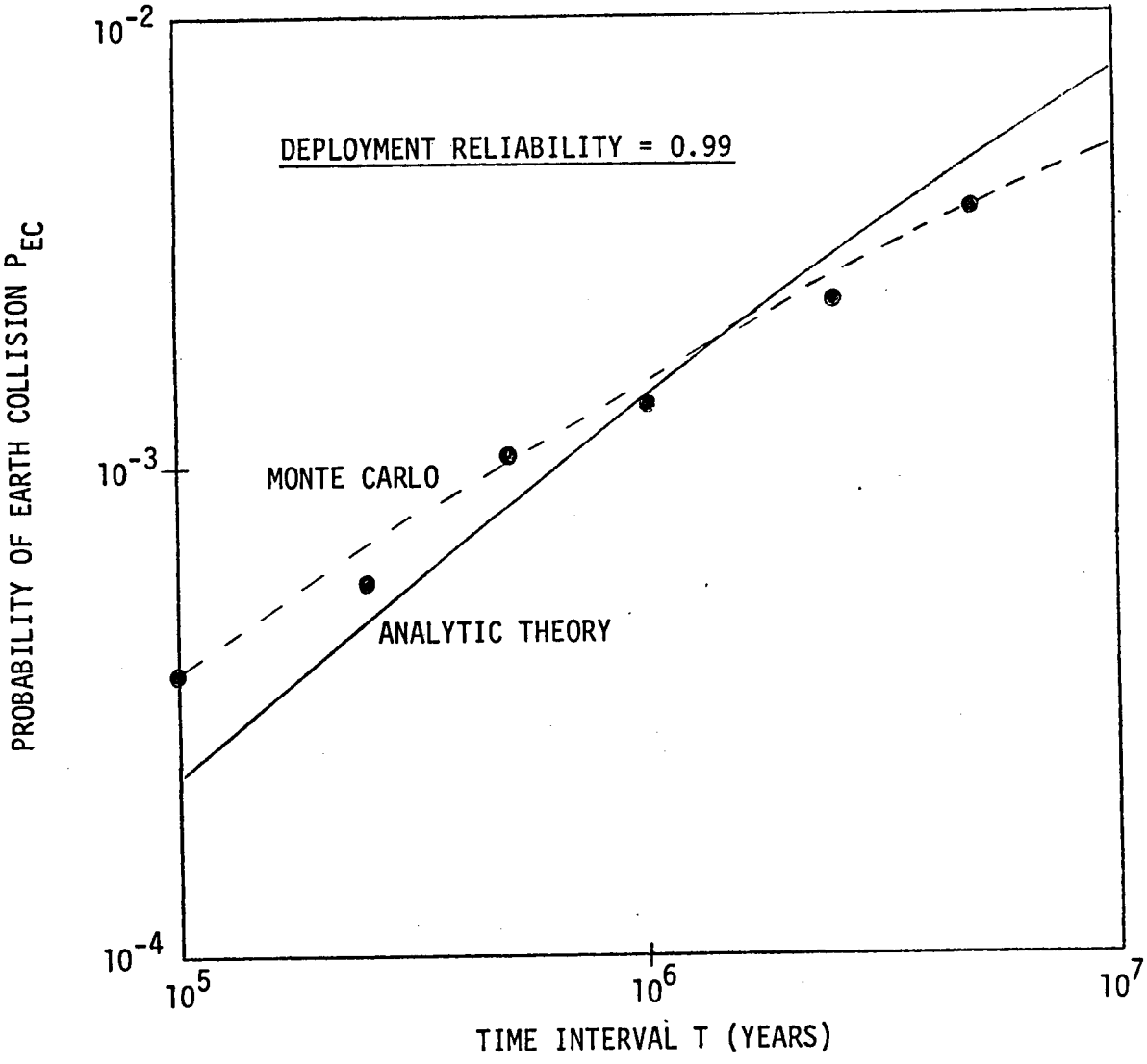

Fig. 3-5 COMPARISON OF ANALYTIC AND MONTE CARLO PREDICTION OF EARTH REENTRY RISK FOR SOLAR SYSTEM ESCAPE MISSION ($i = 0^o$)

Figure 3-6 shows the 10^6 year risk profile as a function of system failure level (1 - R) and the number of "standby" rescue missions (N). The data are calculated by the formula

$$P_{EC}(R,N) = P_{EC}(R,0)[1 - R]^N$$

where $P_{EC}(R,0)$ is the total probability of Earth collision for a single payload launch obtained from the Monte Carlo analysis. For example, with R = 0.99, each additional rescue mission yields 2 orders of magnitude further reduction in collision probability. The shaded area in Figure 3-6 indicates the region of likely interest for mission design. Suppose that the maximum acceptable risk of Earth reentry is 10^{-8} for a single payload.* This risk can be attained with two rescue missions if the reliability level is 0.996, or at most four rescue missions if the reliability is only 0.965. Figure 3-7 shows the risk profile as a function of time over the interval 10^5 to 10^7 years assuming a system reliability level of 99%.

In summary, it has been shown that it is not necessary to have deployment systems of extremely high reliability in order to achieve very low risk. Instead, rescue mission provides this assurance through the powerful mechanism of redundancy. It is suggested that such redundancy on a mission level is likely to be far less costly to obtain than the equivalent redundancy that would be required on a system design level.

---

*e.g., in a total space disposal program consisting of 100 launches, this long-term risk corresponds to only one chance in a million that any payload will reenter Earth's atmosphere.

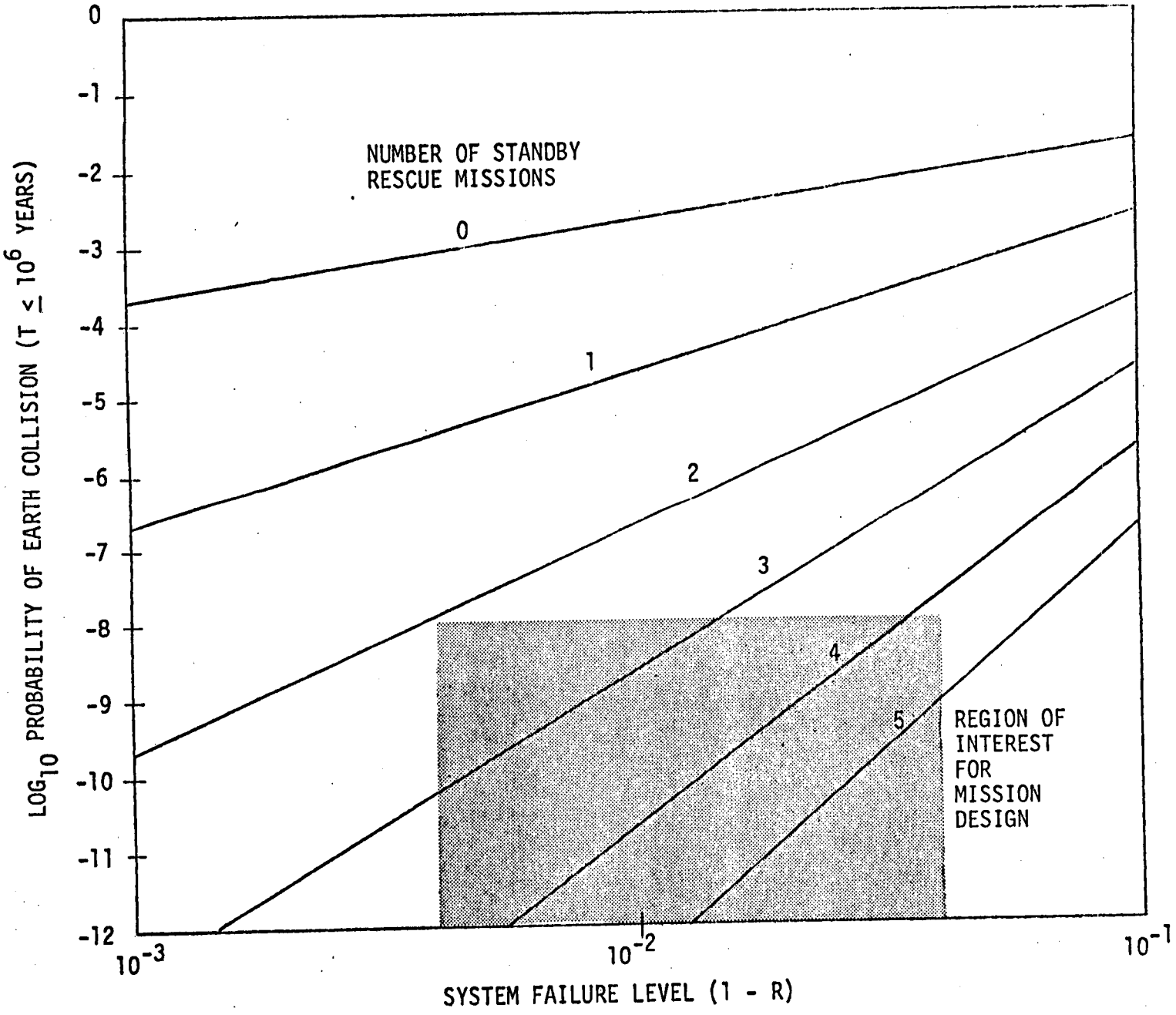

Fig. 3-6 10^6 YEAR RISK PROFILE FOR SOLAR ORBIT DISPOSAL WITH RESCUE CAPABILITY, NOMINAL ORBIT: 0.86 AU CIRCULAR, 2° INCLINATION

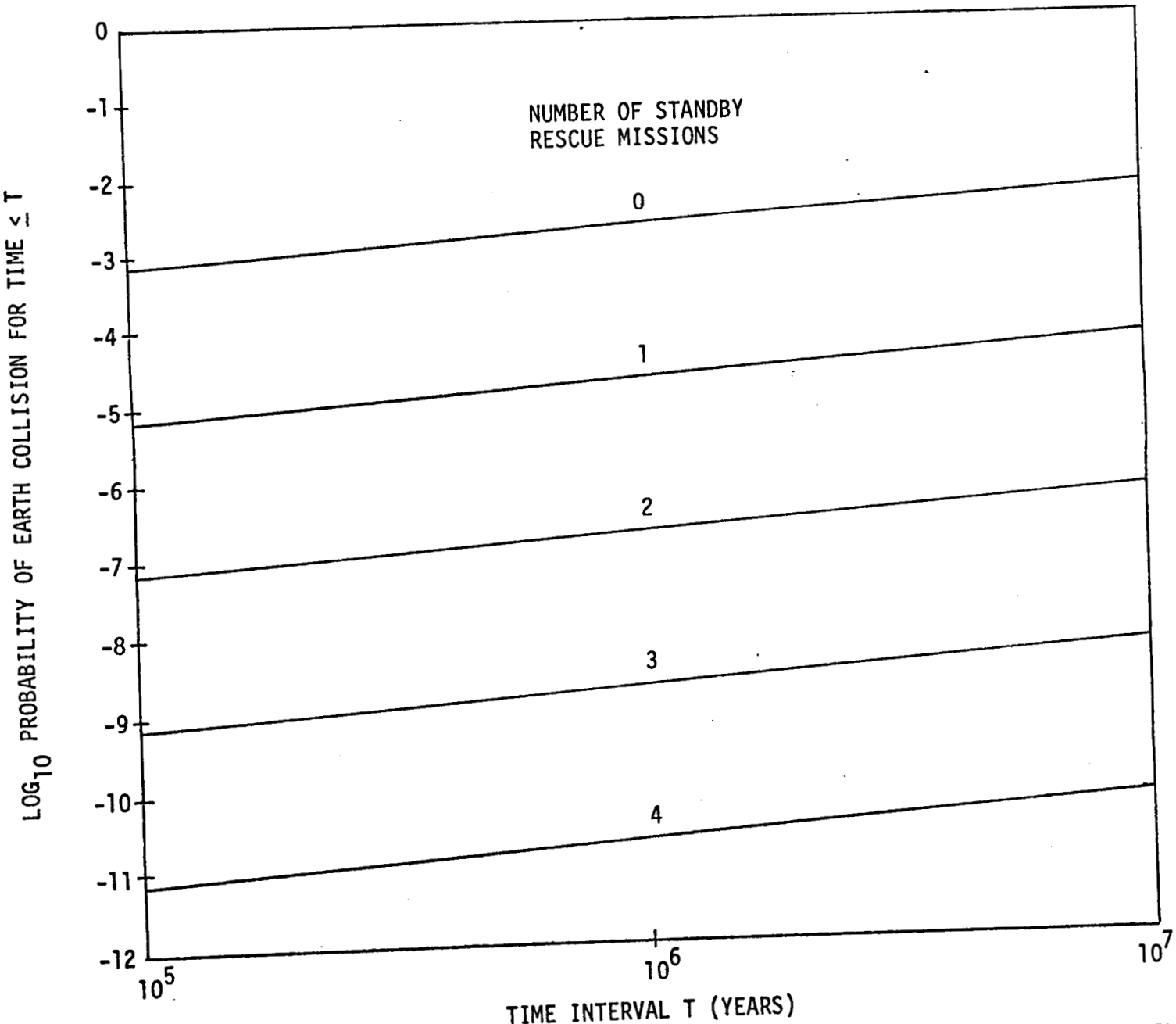

Fig. 3-7 99% RELIABILITY RISK PROFILE FOR SOLAR ORBIT DISPOSAL WITH RESCUE CAPABILITY, NOMINAL ORBIT: 0.86 AU CIRCULAR, 2^o INCLINATION

Section 3 References

3.1 Friedlander, A. L., et al., "Aborted Space Disposal of Hazardous Material: The Long-Term Risk of Earth Reencounter," Science Applications, Inc., Report No. 1-120-676-T8, February 1977.

3.2 Arnold, J. R., "The Origin of Meteorites As Small Bodies," Isotopic and Cosmic Chemistry, 1964, pp. 347-364.

3.3 Arnold, J. R., "The Origin of Meteorites As Small Bodies, II. The Model," Astrophysical Journal, 1965, pp. 1536-1547.

3.4 Wetherill, G. W., "Relationships Between Orbits and Sources of Chondritic Meteorites," Meteorite Research, 1969, pp. 573-589.

3.5 Wetherill, G. W., "Solar System Sources of Meteorites and Large Meteoroids," Annual Reviews of Earth and Planetary Sciences, 1974, pp. 303-331.

4. RESCUE MISSION REQUIREMENTS

For the case of waste disposal in solar storage orbits, the probability that a single failed payload will reentry Earth's atmosphere within a time period 250,000 years after launch is of the order 10^{-3}, i.e., one chance in a thousand. This relatively high level of risk has been stated to be unacceptable by some program planners. However, the analysis described in the previous section has shown that rescue mission capability may be used to reduce this risk to less than 10^{-8}. The question to be addressed then relates to the requirements imposed on such rescue missions.

Consider the following situation and response scenario:

- Situation--due to some deployment system failure, the payload is stranded in an Earth-crossing orbit having a finite probability of reentry in the long term. The payload has not broken apart and it appears likely that a rendezvous/docking operation can be achieved in the short term, i.e., within several years after launch.
- Response--as soon as is practical, launch a rescue mission to retrieve and place the failed payload into a stable solar orbit. If for some reason the rescue mission fails, then launch another--(etc.), thereby assuring the acceptable level of risk against reentry.

Problem areas for study implied by this scenario are: (1) the range of possible failed orbits; (2) rendezvous phasing orbit requirements with rescue time/ΔV trades; (3) rescue propulsion stage requirements with possible constraints on hardware commonality; and (4) automated rendezvous/docking procedures and guidance accuracy.

Figure 4-1 serves to scope the analysis by describing the failure events considered and the range of resulting solar orbits. The desired target orbit is circular at 0.86 AU and inclined to the ecliptic plane

by a small angle, nominally 2°. Injection to the 0.86 × 1.0 AU transfer orbit is performed by a reusable OTV propulsion system, and circularization at 0.86 AU (6 months later) is accomplished by a kick stage injected with the payload. Three failure modes occurring after Earth escape condition* ($C_3 = 0$) can leave the payload in an unstable solar orbit. In the first instance, a late OTV failure, the proper response is to immediately start up the kick stage to implement completion of the nominal injection to the 0.86 × 1.0 AU transfer orbit. For corrective maneuvers within 20,000 km altitude above the Earth, the required ΔV is less than 100 m/sec. Since this is within the propellant budget of the baseline kick stage, there is no further reason to consider this particular failure/corrective mode--assuming of course that the kick stage does not fail. The two remaining cases of interest then are: (1) sequential failure of both OTV and kick stages at injection leaving the payload in an orbit with aphelion distance of 1.0 AU and perihelion distance somewhere in the range 1.0 to 0.86 AU depending on the time of failure; and (2) successful OTV burn but kick stage failure during the circularization maneuver leaving the payload in an orbit with perihelion 0.86 AU and aphelion somewhere in the range 1.0 to 0.86 AU.

In the first case above, a rescue mission is clearly needed since both nominal propulsion stages are inoperable. In the second case, a rescue mission is required if the kick stage fails at startup, but may not be needed if the aphelion distance is sufficiently close to 0.86 AU as a result of a late kick stage failure. Rather than restrict the analysis by such implied operational decisions, we will examine the rescue ΔV requirements over the entire range of orbit dimensions. However, we will return to the question of orbit stability for situations of off-nominal, but non-Earth crossing solar orbits.

---

*Failure occurrences prior to achieving Earth escape will leave the waste payload in an Earth-bound orbit. Rescue requirements for this situation are being studied by MSFC and Battelle.

Fig. 4-1

FAILURE EVENTS AND RESULTING ORBITS

- NOMINAL DEPLOYMENT TO SOLAR ORBIT
  - OTV INJECTION TO 0.86 × 1.0 AU TRANSFER ORBIT
  - KICK STAGE CIRCULARIZATION AT 0.86 AU

- LATE OTV FAILURE (BEYOND EARTH-ESCAPE ENERGY)
  - START UP KICK STAGE TO COMPLETE INJECTION (ΔV < 100 M/SEC)

- OTV AND KICK STAGE FAILURE AT R = 1.0 AU
  - ORBIT APHELION: 1.0 AU
  - ORBIT PERIHELION: 1.0 - 0.86 AU

- KICK STAGE FAILURE AT R = 0.86 AU
  - ORBIT PERIHELION: 0.86 AU
  - ORBIT APHELION: 1.0 - 0.86 AU

4.1 Rendezvous Phasing Orbits

The first step in the analysis is to calculate the minimum ΔV requirement assuming a time-independent optimal phasing situation and no additional loss due to finite thrust penalty or terminal rendezvous maneuvers. This establishes a reference data base against which real maneuver requirements can be assessed. Results are shown in Figure 4-2. The first velocity impulse, ΔV_1, is provided by the rescue OTV at Earth parking orbit injection. Over the range of orbits at 2° inclination, the ΔV_1 requirement is approximately constant (3.25 to 3.31 km/sec); the equivalent launch energy C_3 range is 1.08 to 2.35 km^2/sec^2. The remaining impulses, ΔV_2 and ΔV_3, are provided by the rescue kick stage. The right-hand graph which depicts failure mode #1 shows an ideal "free" rendezvous and a placement ΔV varying from the nominal value of 1.187 km/sec to 2.330 km/sec. Failure mode #2 is shown in the left-hand graph. In this case, the sum $\Delta V_2 + \Delta V_3$ is always equal to 1.187 km/sec; i.e., the total ΔV requirement is independent of aphelion distance. To summarize, over the range of possible rescue orbits the minimum total ΔV requirement varies from 4.5 to 5.7 km/sec depending on the orbit size.

It is possible to approach the ideal phasing conditions as closely as desired if one is willing to wait the requisite amount of time before mounting the rescue mission. Although it is true that the near-term risk of Earth reentry is negligible, there may be a practical desire to mount an early rescue mission; e.g., to take advantage of a still-functioning communications and attitude control system on the failed payload in order to cooperate in the rescue operations. It is important, at least, to identify the ΔV tradeoff with time. Figure 4-3 shows such a tradeoff for a failed payload in a 0.86 × 1.0 AU orbit with arbitrary inclination. Results are given in terms of ΔV penalty above the minimum ΔV requirement, but again assuming no losses other than orbit phasing. The left-hand graph applies to rendezvous and placement at 0.86 AU, while the right-hand graph assumes rendezvous at 1.0 AU and placement ∿0.45 years later at 0.86 AU. Data is shown for launching the rescue mission from 0.5 to 2 years

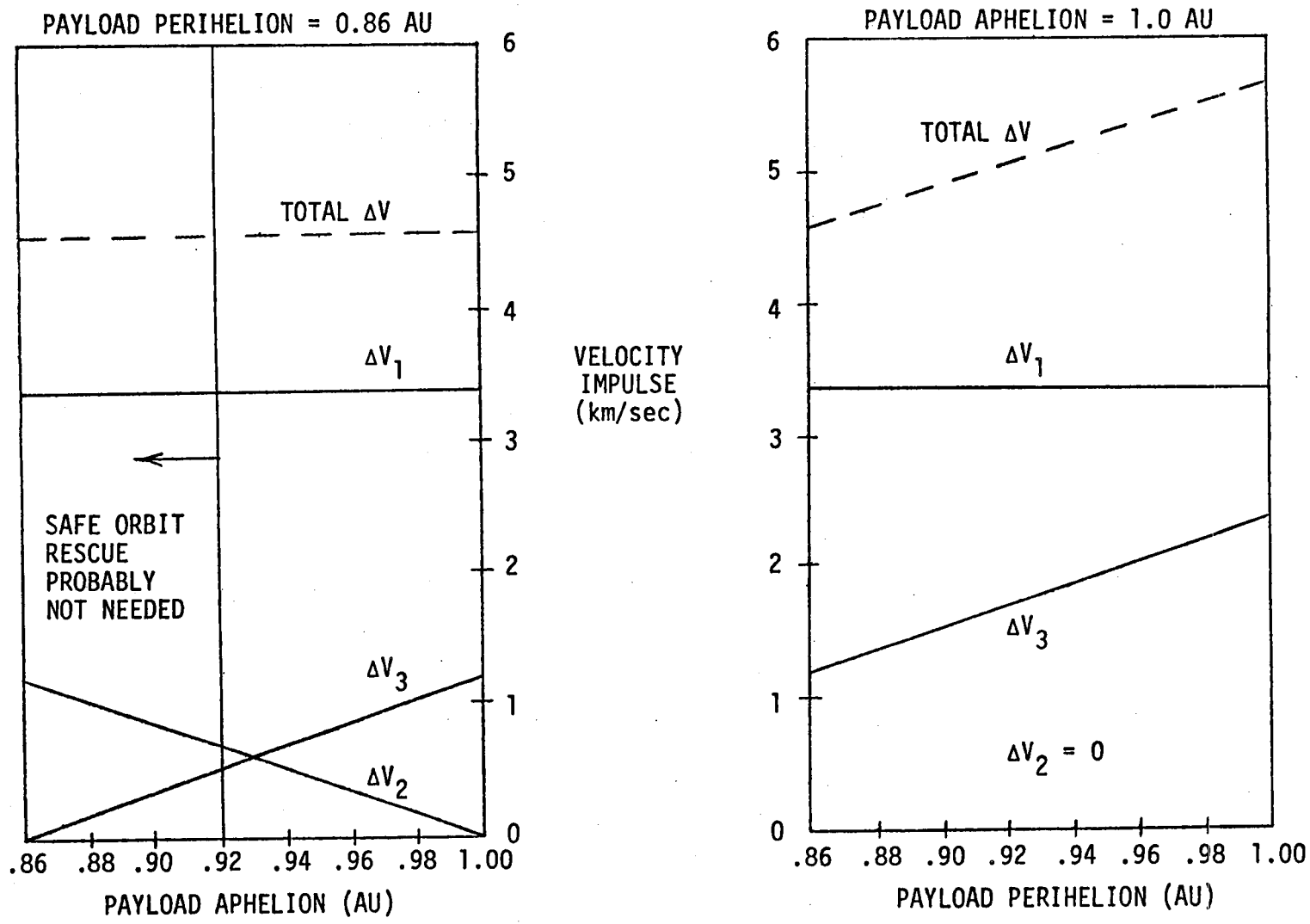

Fig. 4-2 MINIMUM (OPTIMAL PHASING) ΔV REQUIREMENTS FOR SOLAR ORBIT RESCUE

ΔV_1 = PARKING ORBIT INJECTION; ΔV_2 = RENDEZVOUS; ΔV_3 = PLACEMENT

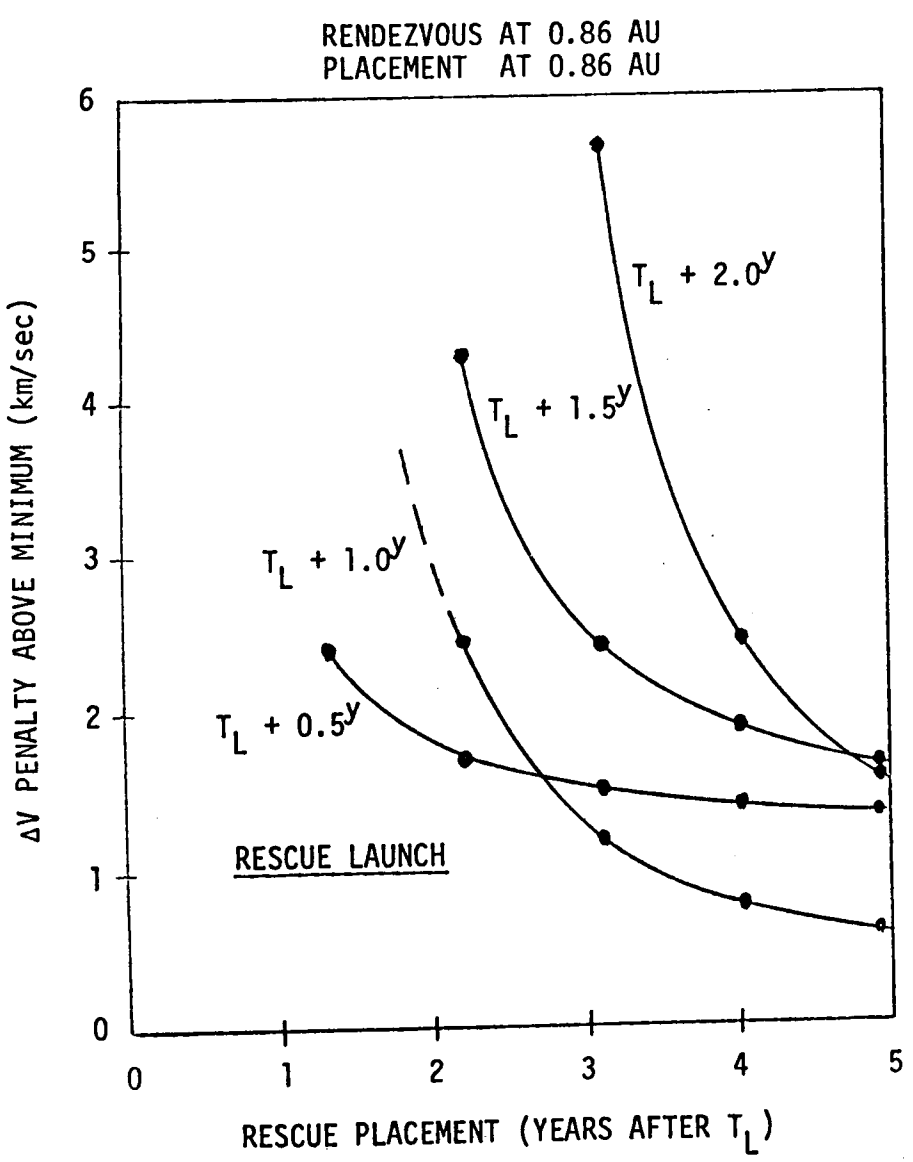

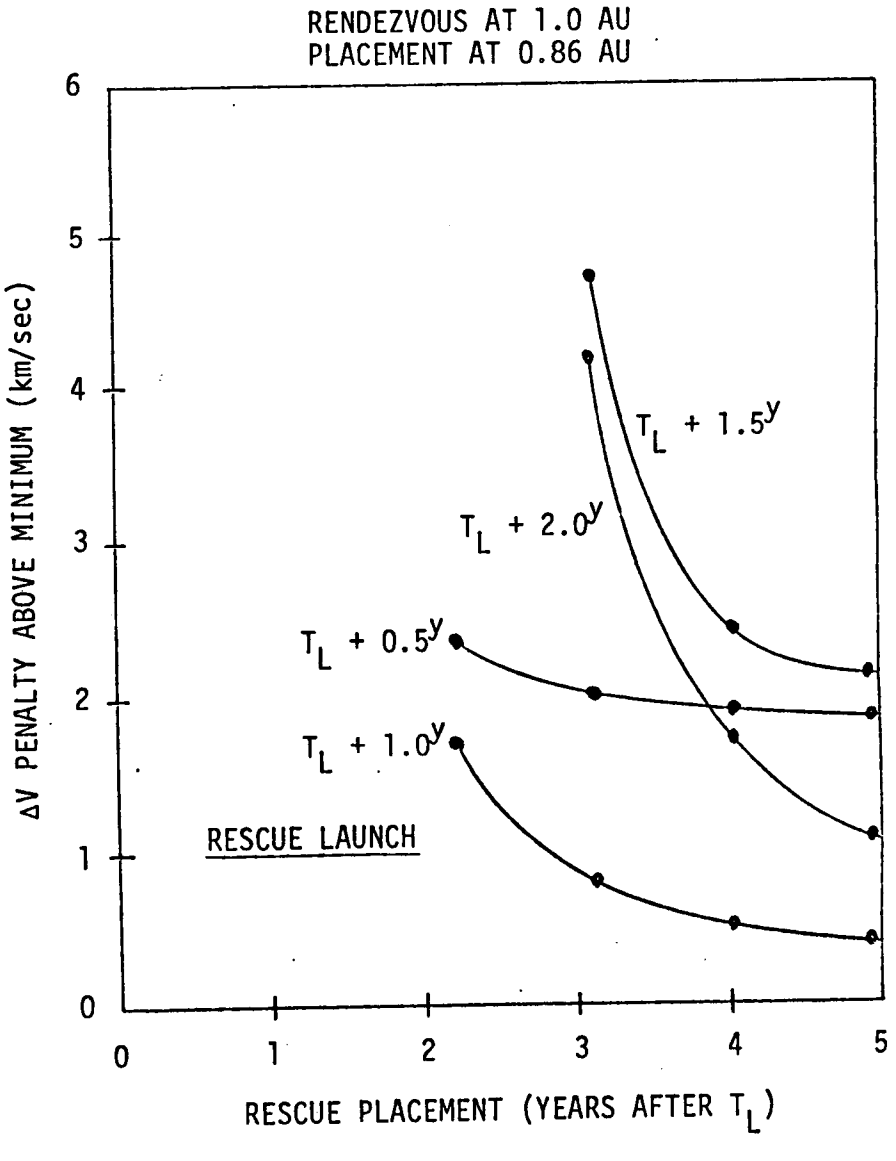

Fig. 4-3 REAL PHASING ΔV PENALTY FOR SOLAR ORBIT RESCUE (T_L = PAYLOAD LAUNCH DATE)
ASSUMING PAYLOAD ORBIT = 0.86 × 1.0 AU, PLACEMENT ORBIT = 0.86 AU CIRCULAR

after the original payload launch date, and placement time up to 5 years after payload launch. It should be noted that rescue launch at $T_L + 0.5^y$ allows for only a 3 week period between first indication of kick stage failure and rescue launch, implying an "on-the-pad" readiness. This short response is not inconsistent with the possible need to quickly rescue a failed payload in Earth orbit. Another point to note is that only the solid dot data points correspond to specific rescue mission scenarios.

Launches at half-year intervals are more efficient if rendezvous takes place at 0.86 AU, whereas a 1.0 AU rendezvous is better for launches at 1 year intervals. Also, for placement within 5 years, it is best to launch the rescue mission early, i.e., within the first year. The earliest placement, at 1.35 years, requires an immediate rescue mission having a ΔV penalty of 2.402 km/sec. Otherwise, the rescue mission launched at $T_L + 1^y$ with rendezvous at 1.0 AU provides a minimum ΔV penalty from 1.693 to 0.369 km/sec.

4.2 Propulsion Stage Requirements

Rescue mission ΔV requirements are translated to propulsion system performance using the mass characteristics data provided by MSFC. This data listed in Table 4-1 assumes that the rescue mission is implemented by propulsion hardware similar to that used for the nominal payload launch. In most cases, a reusable OTV will be employed for the rescue injection and one or more kick stages used for implementing the rendezvous, orbit transfer and placement maneuvers. The nuclear waste payload is assumed to weigh 10,495 lb. Performance calculations include a 100 m/sec allowance for terminal rendezvous maneuvers and finite thrust losses, and assume that use of attitude control propellant is equally split between pre-rendezvous and pre-placement maneuvers. Another important assumption is that the failed kick stage is jettisoned after rendezvous; it would be very inefficient to have to carry this "dead weight."

Table 4-1

MASS CHARACTERISTICS DATA

• REUSABLE OTV			
SPECIFIC IMPULSE	470 sec		
STAGE INERT WEIGHT	6,370 lbs		
INJECTED WEIGHT	27,004 lbs	@	$C_3 = 1.3$
	22,674 lbs	@	$C_3 = 3.5$
• KICK STAGE (MMH/N_2O_4)			
SPECIFIC IMPULSE	289 sec		
STAGE INERT WEIGHT	2,860 lbs	}	11,943 lbs
ACS PROPELLANT	254 lbs	}	
MAIN PROPELLANT	8,829 lbs	}	
• NUCLEAR WASTE PAYLOAD	10,495 lbs		
• PERFORMANCE CALCULATION ASSUMPTIONS			
MANEUVER LOSSES	100 m/sec		
ACS USAGE	50% pre-rendezvous, 50% pre-placement		
FAILED KICK STAGE	jettison after rendezvous		

Several failure scenarios covering the spectrum of Earth-crossing orbit conditions were postulated and details of possible rescue responses were calculated in terms of the ΔV and propulsion stage requirements. Results of these failure case studies are presented in Table 4-2. Rescue stage requirements shown reflect the desired placement into the nominal circular stable orbit at 0.86 AU within 5 years of the original payload launch. This may necessitate the use of two baseline kick stages as noted in Cases 1 (Alternative), 2A, 2B and 3A. It is always possible, of course, to design a single, larger propulsion stage to accomplish the rescue mission. However, this implies the use of nonstandard hardware and may be less cost-effective than using two standard kick stages.

One exception to using the standard reusable OTV is shown for failure Case 1 in which the payload is left in a 1.0 × 1.0 AU orbit. In this case an expendable OTV is considered for rendezvous and transfer ΔV implementation, and a single kick stage performs the final placement maneuver. The cryogenic propellant in the OTV must be stored for a longer than usual time interval, but probably not exceeding 10 days of operation in the near vicinity of Earth.

There is an attractive alternative to consider when a single baseline kick stage is insufficient to recapture the nominal 0.86 AU circular orbit. That is, the available ΔV capability could be used to establish a circular orbit at some other distance or a slightly elliptical orbit. Data for this alternative option are presented as footnotes in Table 4-2. If these fallback orbits exhibit a sufficient measure of stability against planet perturbations, then it should be possible to perform all rescue missions with a single baseline kick stage. Figure 4-4 shows the variation of orbit distance for an initially circular orbit at 0.90 AU which encompasses the fallback options noted for Cases 2A and 2B. The storage orbit aphelion distance does barely cross Earth's perihelion, but not until a time interval of 600,000 years has elapsed. Hence, the 0.90 AU circular orbit could be said to possess at least marginal long-term stability. Additional results are shown in Figures 4-5 through 4-7

Table 4-2

RESCUE MISSION PROPULSION REQUIREMENTS - CASE STUDIES

CASE NUMBER: .1

FAILURE EVENT: OTV and kick stage failure at T_L
Payload in orbit 1.0 × 1.0 AU, I = 2°

RESCUE RESPONSE: Launch expendable OTV and baseline kick stage
Use OTV for rendezvous and transfer ΔV
Use kick stage for placement 0.86 AU circular

RESCUE SCENARIO:

Event	Time	Distance	C_3 or ΔV
Inject to Earth escape	$T_L + (N/2)^y$	1.0 AU	C_3 = 1.08 @ I = 2°
Rendezvous and dock	$\sim 10^d$ later	1.0	ΔV = 0.100 km/sec
Transfer to 0.86 × 1.0 AU	same	1.0	1.143
Placement	$\sim 0.45^y$ later	0.86	1.187

STAGE REQUIREMENTS:

Stage Number	ΔV (km/sec)	Propellant (lbs)
1 (Expendable OTV)	4.656	44687 (41645 used)
2 (Baseline Kick)	1.187	8829 (7591 used)

TOTAL INJECTED WEIGHT: 51057 + 11943 = 63000 lbs
in 300 km Earth parking orbit
30043 lbs to C_3 = 1.08

TOTAL RESCUE MISSION TIME: 0.45 years

Table 4-2 (cont'd.)

RESCUE MISSION PROPULSION REQUIREMENTS - CASE STUDIES

CASE NUMBER: 1 (Alternative)

FAILURE EVENT: OTV and kick stage failure at T_L
Payload in orbit 1.0 × 1.0 AU, I = 2°

RESCUE RESPONSE: Launch two** baseline kick stages
Establish best possible stable orbit,
0.86 × 0.873 AU*

RESCUE SCENARIO:

Event	Time	Distance	C_3 or ΔV
Inject to Earth escape	$T_L + (N/2)^y$	1.0 AU	C_3 = 1.08 @ I = 2°
Rendezvous and dock	$\sim 10^d$ later	1.0	ΔV = 0.100 km/sec
Transfer to 0.86 × 1.0 AU	same	1.0	1.143
Placement	$\sim 0.45^y$ later	0.86	1.066*

STAGE REQUIREMENTS:

Stage Number	ΔV (km/sec)	Propellant (lbs)
1 (Baseline Kick)	0.875	8829 (8829 used)
2 (Baseline Kick)	1.434	8829 (8829 used)

TOTAL INJECTED WEIGHT: 2 × 11943 = 23886 lbs to C_3 = 1.08

TOTAL RESCUE MISSION TIME: 0.45 years

*Insufficient ΔV capability of 1.187 - 1.066 = 0.121 km/sec.
**Second alternative using only single kick stage is placement into circular orbit 0.915 × 0.915 AU.

Table 4-2 (cont'd.)

RESCUE MISSION PROPULSION REQUIREMENTS - CASE STUDIES

CASE NUMBER: 2A (Placement at $T_L + 2.344^y$)

FAILURE EVENT: OTV and kick stage failure at T_L
Payload in orbit 0.93 × 1.0 AU, I = 2°

RESCUE RESPONSE: Launch two* baseline kick stages for rendezvous, transfer and placement 0.86 AU circular

RESCUE SCENARIO:

Event	Time	Distance	C_3 or ΔV
Inject to 0.859 × 1.0 AU orbit	$T_L + 1.0^y$	1.0 AU	C_3 = 2.34 @ I = 2°
Wait one revolution			
Rendezvous and dock	$T_L + 1.896^y$	1.0	ΔV = 0.710 km/sec
Transfer to 0.86 × 1.0 AU	$T_L + 1.896^y$	1.0	0.598
Placement	$T_L + 2.344^y$	0.86	1.187

STAGE REQUIREMENTS:

Stage Number	ΔV (km/sec)	Propellant (lbs)
1 (Baseline Kick)	1.083	8829 (8829 used)
2 (Baseline Kick)	1.412	8829 (8718 used)

TOTAL INJECTED WEIGHT: 2 × 11943 = 23886 lbs to C_3 = 2.34

TOTAL RESCUE MISSION TIME: 1.344 years

*Alternative using only single kick stage is placement into circular orbit 0.90 × 0.90 AU, or elliptical orbit 0.86 × 0.941 AU.

Table 4-2 (cont'd.)

RESCUE MISSION PROPULSION REQUIREMENTS - CASE STUDIES

CASE NUMBER: 2B (Placement at $T_L + 4.240^y$)

FAILURE EVENT: OTV and kick stage failure at T_L
Payload in orbit 0.93 × 1.0 AU, I = 2°

RESCUE RESPONSE: Launch two* baseline kick stages for rendezvous, transfer and placement 0.86 AU circular

RESCUE SCENARIO:

Event	Time	Distance	C_3 or ΔV
Inject to 0.906 × 1.0 AU orbit	$T_L + 1.0^y$	1.0 AU	C_3 = 1.61 @ I = 2°
Wait three revolutions			
Rendezvous and dock	$T_L + 3.792^y$	1.0	ΔV = 0.295 km/sec
Transfer to 0.86 × 1.0 AU	$T_L + 3.792^y$	1.0	0.598
Placement	$T_L + 4.240^y$	0.86	1.187

STAGE REQUIREMENTS:

Stage Number	ΔV (km/sec)	Propellant (lbs)
1 (Baseline Kick)	0.893	8829 (8397 used)
2 (Baseline Kick)	1.187	8829 (7591 used)

TOTAL INJECTED WEIGHT: 2 × 11943 = 23886 lbs to C_3 = 1.61

TOTAL RESCUE MISSION TIME: 3.240 years

*Alternative using only single kick stage is placement into circular orbit 0.888 × 0.888 AU, or elliptical orbit 0.86 × 0.917 AU.

Table 4-2 (cont'd.)

RESCUE MISSION PROPULSION REQUIREMENTS - CASE STUDIES

CASE NUMBER: 3A (Placement at $T_L + 2.242^y$)

FAILURE EVENT: Kick stage failure at $T_L + 0.448^y$
Payload in orbit 0.86 × 1.0 AU, I = 2°

RESCUE RESPONSE: Launch two* baseline kick stages for rendezvous and placement 0.86 AU circular

RESCUE SCENARIO:

Event	Time	Distance	C_3 or ΔV
Inject to 0.715 × 1.0 AU orbit	$T_L + 1.0^y$	1.0 AU	C_3 = 7.71 @ I = 2°
Wait one revolution			
Rendezvous and dock	$T_L + 1.794^y$	1.0	ΔV = 1.460 km/sec
Placement	$T_L + 2.242^y$	0.86	1.187

STAGE REQUIREMENTS:

Stage Number	ΔV (km/sec)	Propellant (lbs)
1 (Baseline Kick)	1.460	8829 (8808 used)
2 (Baseline Kick)	1.187	6947 (6947 used)

TOTAL INJECTED WEIGHT: 11943 + 10061 = 22004 lbs to C_3 = 7.71

TOTAL RESCUE MISSION TIME: 1.242 years

*Alternative using only single kick stage is placement into elliptical orbit 0.86 × 0.908 AU.

Table 4-2 (cont'd.)

RESCUE MISSION PROPULSION REQUIREMENTS - CASE STUDIES

CASE NUMBER: 3B (Placement at $T_L + 4.933^y$)

FAILURE EVENT: Kick stage failure at $T_L + 0.448^y$
Payload in orbit 0.86 × 1.0 AU, I = 2°

RESCUE RESPONSE: Launch one baseline kick stage for rendezvous and placement 0.86 AU circular

RESCUE SCENARIO:

Event	Time	Distance	C_3 or ΔV
Inject to 0.824 × 1.0 AU orbit	$T_L + 1.0^y$	1.0 AU	C_3 = 3.20 @ I = 2°
Wait four revolutions			
Rendezvous and dock	$T_L + 4.484^y$	1.0	ΔV = 0.429 km/sec
Placement	$T_L + 4.933^y$	0.86	1.187

STAGE REQUIREMENTS:

Stage Number	ΔV (km/sec)	Propellant (lbs)
1 (Baseline Kick)	1.616	8829 (8683 used)

TOTAL INJECTED WEIGHT: 11943 lbs to C_3 = 3.2

TOTAL RESCUE MISSION TIME: 3.933 years

Table 4-2 (cont'd.)

RESCUE MISSION PROPULSION REQUIREMENTS - CASE STUDIES

CASE NUMBER: 4A (Placement at $T_L + 2.989^y$)

FAILURE EVENT: Kick stage failure at $T_L + 0.448^y$
Payload in orbit 0.86 × 0.93 AU, I = 2°

RESCUE RESPONSE: Launch one baseline kick stage for transfer, rendezvous and placement 0.86 AU circular

RESCUE SCENARIO:

Event	Time	Distance	C_3 or ΔV
Inject to 0.750 × 1.0 AU orbit	$T_L + 1.0^y$	1.0 AU	C_3 = 5.88 @ I = 2°
Transfer to 0.750 × 0.93 AU	$T_L + 1.409^y$	0.750	ΔV = 0.579 km/sec
Wait 1.5 revolutions			
Rendezvous and dock	$T_L + 2.565^y$	0.93	1.191
Placement	$T_L + 2.989^y$	0.86	0.622

STAGE REQUIREMENTS:

Stage Number	ΔV (km/sec)	Propellant (lbs)
1 (Baseline Kick)	2.392	8829 (8779 used)

TOTAL INJECTED WEIGHT: 11943 lbs to C_3 = 5.88

TOTAL RESCUE MISSION TIME: 1.989 years

Table 4-2 (cont'd.)

RESCUE MISSION PROPULSION REQUIREMENTS - CASE STUDIES

CASE NUMBER: 4B (Placement at $T_L + 4.681^y$)

FAILURE EVENT: Kick stage failure at $T_L + 0.448^y$
Payload in orbit 0.86 × 0.93 AU, I = 2°

RESCUE RESPONSE: Launch one baseline kick stage for transfer, rendezvous and placement 0.86 AU circular

RESCUE SCENARIO:

Event	Time	Distance	C_3 or ΔV
Inject to 0.805 × 1.0 AU orbit	$T_L + 1.0^y$	1.0 AU	C_3 = 3.76 @ I = 2°
Transfer to 0.805 × 0.93 AU	$T_L + 1.429^y$	0.805	ΔV = 0.572 km/sec
Wait 3.5 revolutions			
Rendezvous and dock	$T_L + 4.258^y$	0.93	0.623
Placement	$T_L + 4.681^y$	0.86	0.622

STAGE REQUIREMENTS:

Stage Number	ΔV (km/sec)	Propellant (lbs)
1 (Baseline Kick)	1.817	8829 (7636 used)

TOTAL INJECTED WEIGHT: 11943 lbs to C_3 = 3.76

TOTAL RESCUE MISSION TIME: 3.681 years

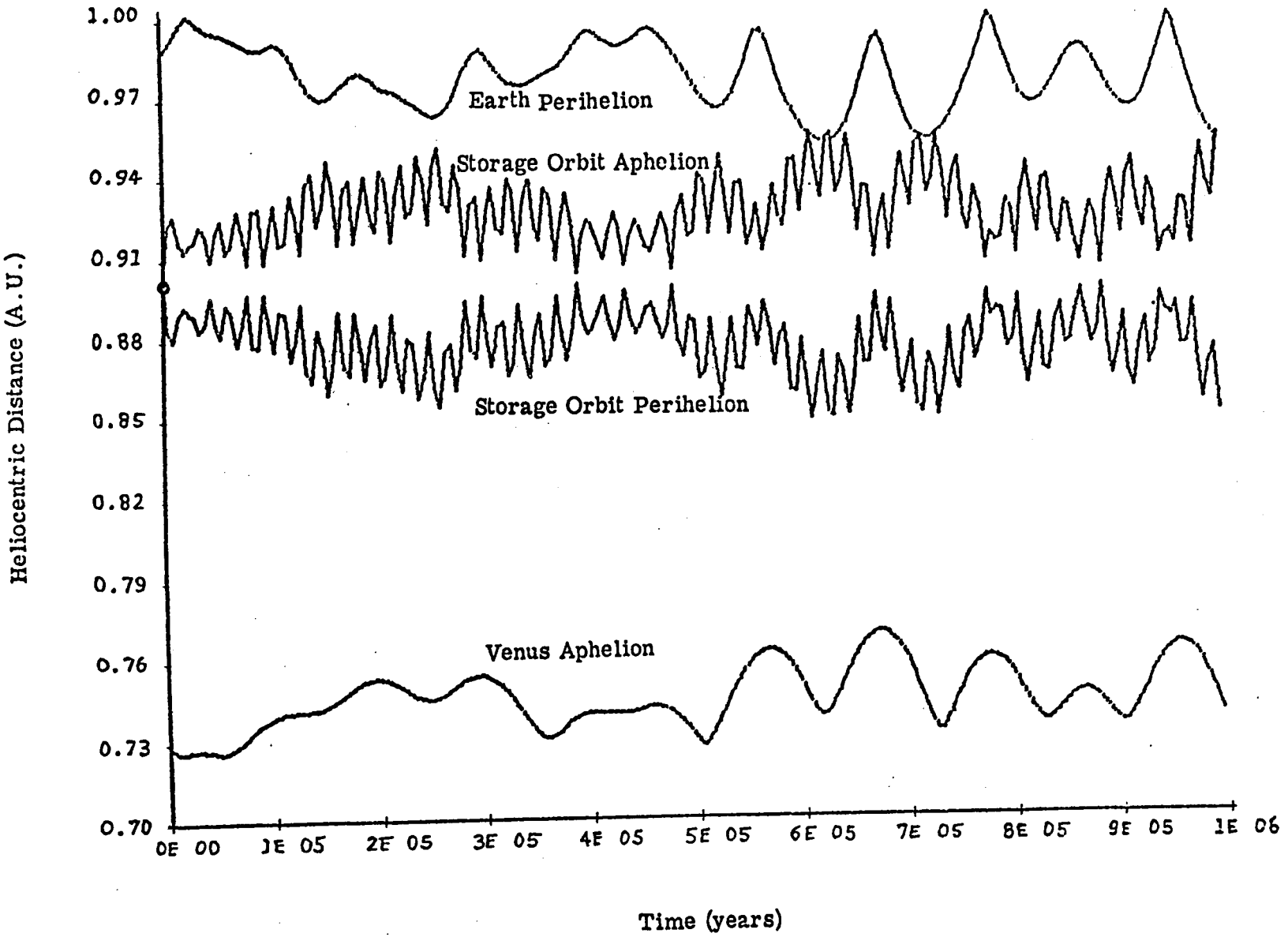

Fig. 4-4 ORBITAL VARIATIONS FOR THE INITIAL ORBIT a = 0.90 AU, e = 0, i = 2^{o}

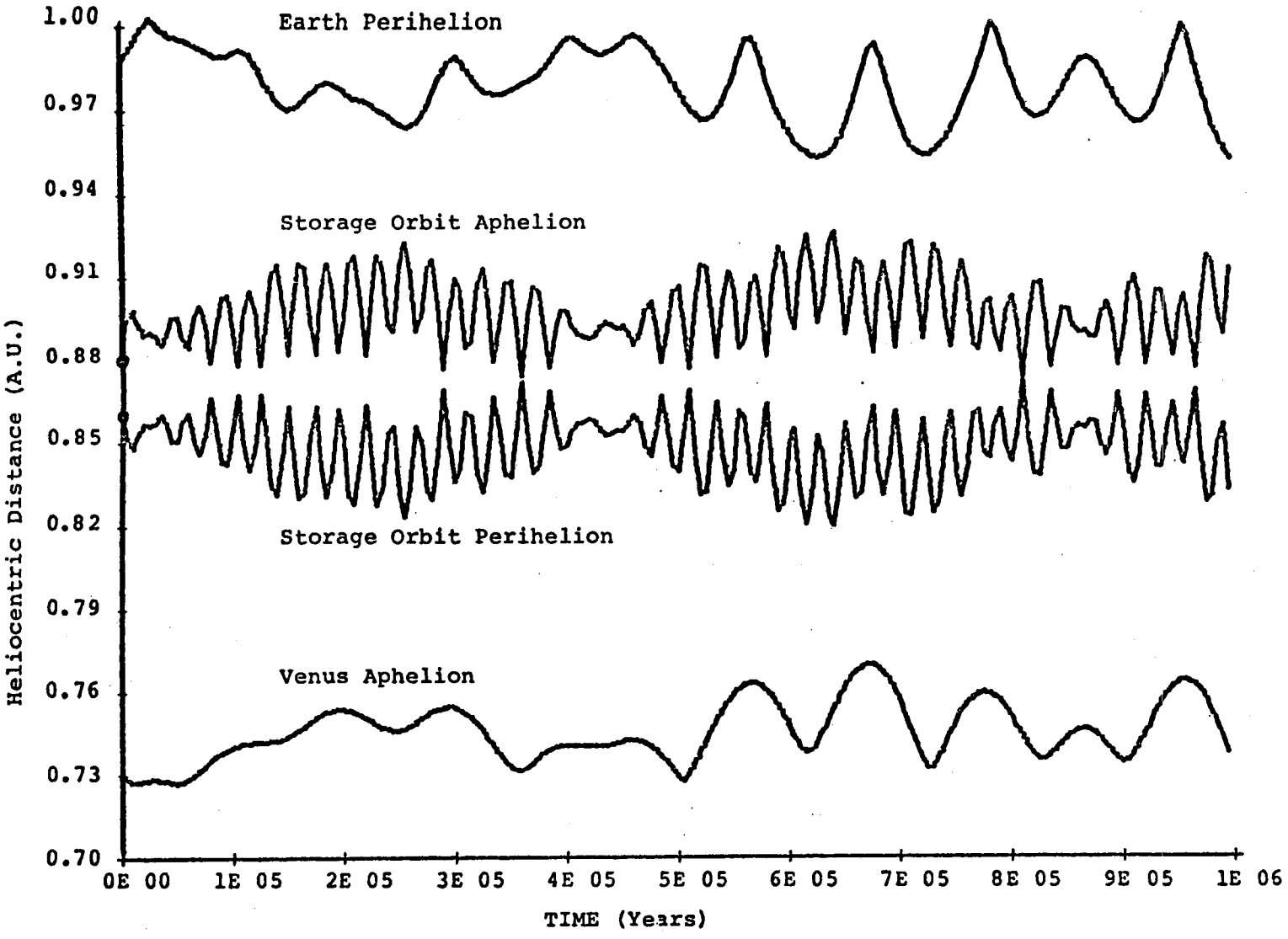

Fig. 4-5 ORBITAL VARIATIONS FOR THE INITIAL ORBIT a = 0.87 AU, e = 0.0115, i = 2^{o}

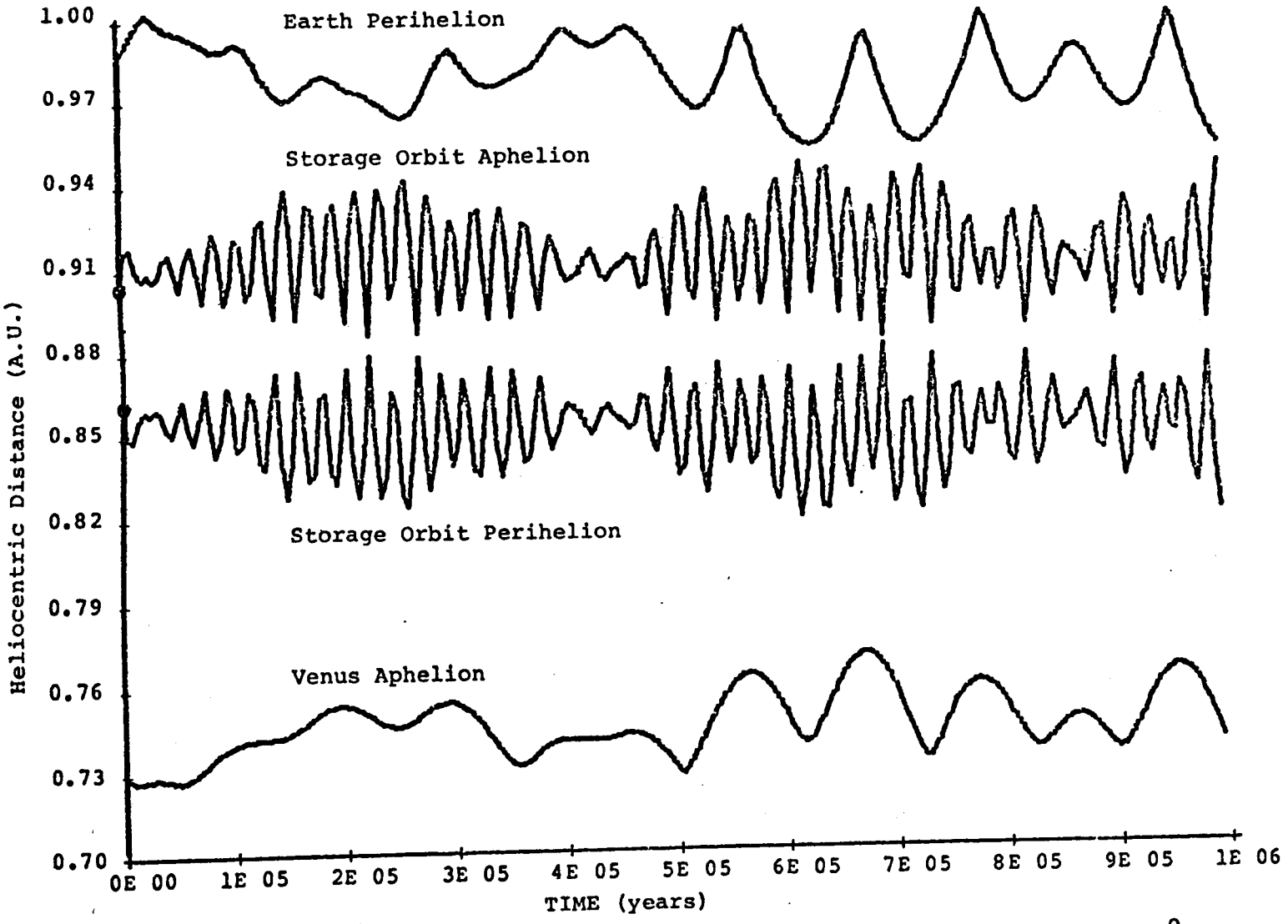

Fig. 4-6 ORBITAL VARIATIONS FOR THE INITIAL ORBIT a = 0.88 AU, e = 0.0227, i = 2^{o}

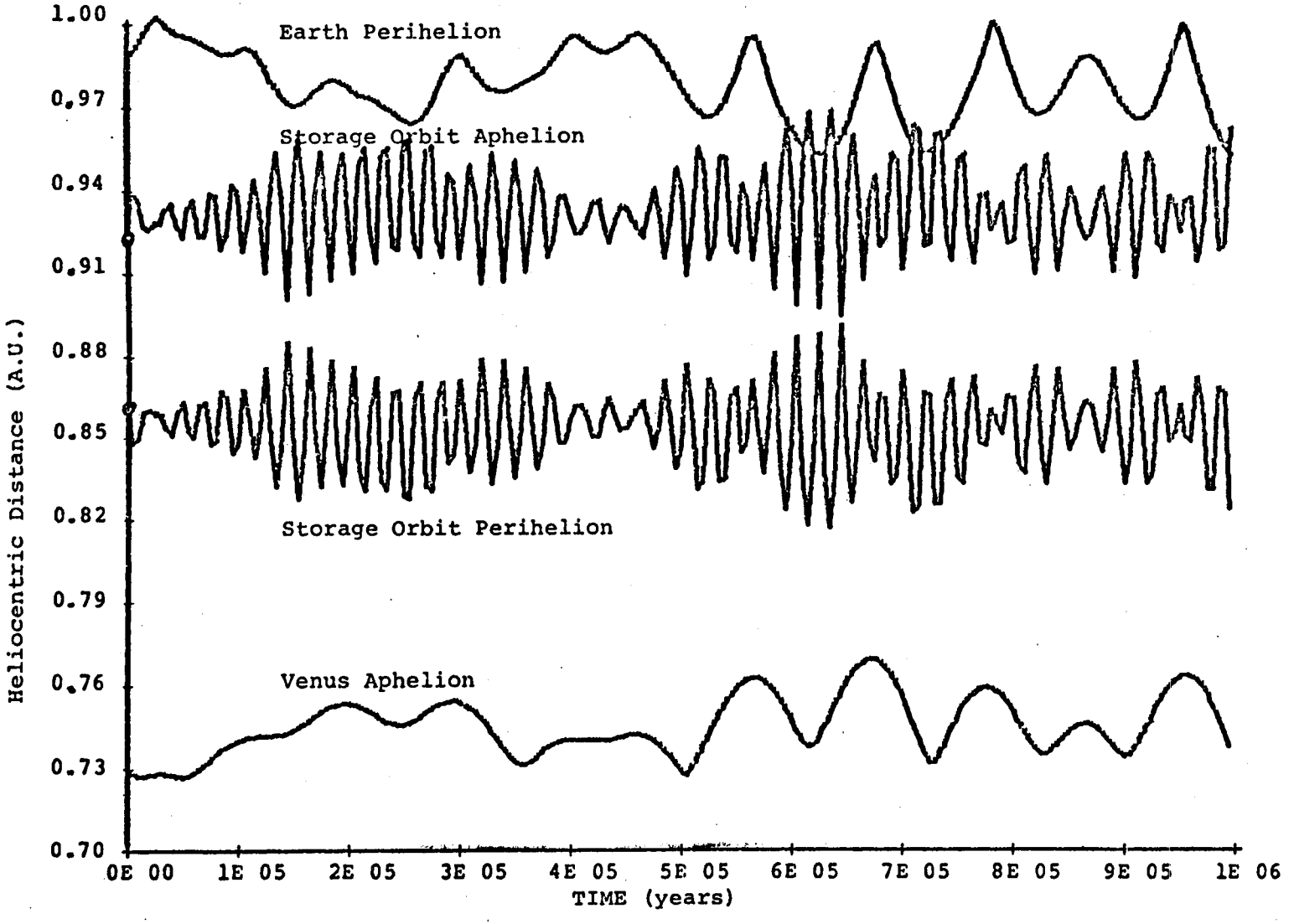

Fig. 4-7 ORBITAL VARIATIONS FOR THE INITIAL ORBIT a = 0.89 AU, e = 0.0337, i = 2^0

for three slightly elliptical initial orbits: 0.86 × 0.88, 0.86 × 0.90, and 0.86 × 0.92 AU. These orbits also appear to be stable for periods up to 10^6 years or, at worst, marginally cross the Earth's orbit for brief intervals during this period. We would conclude, therefore, on the basis of these results obtained from secular perturbation theory, that alternative options do exist for placement of failed payloads into off-nominal stable orbits.

4.3 Automated Rendezvous/Docking Assessment

The most critical aspect of rescue missions is undoubtedly the ability to rendezvous and dock with a payload in deep space. The rescue vehicle must be transfered to the near vicinity of the payload position, close enough to obtain radar acquisition of the target. It must then be very accurately guided during the terminal rendezvous phase through final closure with the target. Lastly, a secure dock must be accomplished in an automated mode. While these maneuvers are not yet commonplace in the space program, there does exist a background of experience and technological development which allows one to project this as an engineering problem that can be solved. The Soviets have already demonstrated automated rendezvous and docking in Earth-Moon space. The U.S. program includes analysis and design experience related to backup options for manned space flight and, more recently, studies related to Mars sample return missions [1] and teleoperator control of Skylab's orbit decay problem [3].

Some of the more salient features and requirements of rescue operations are outlined in Figure 4-8. The most important requirement is that the target vehicle should be able to play some cooperative role in the operations. Earth-based radio tracking of the target orbit for purposes of transfer guidance implies an operable communications link, at least in the transponder section of the payload's communication system. A transponder function is also needed to relay the rescue vehicle's radar

Fig. 4-8

AUTOMATED RENDEZVOUS AND DOCKING IN SOLAR ORBIT

- PREVIOUS EXPERIENCE
  - PRACTICAL IMPLEMENTATION BY SOVIETS IN EARTH-MOON SPACE
  - ANALYSIS AND DESIGN BY U.S. (MANNED PROGRAM, MARS SAMPLE RETURN)

- MOST SIGNIFICANT FEATURES
  - SOME LEVEL OF COOPERATION BY TARGET VEHICLE--OTHERWISE, NEW TECHNOLOGY REQUIREMENTS ASSESSED VERY DIFFICULT
  - HIGH ACCURACY TERMINAL GUIDANCE BY RESCUE VEHICLE
  - ADEQUATE WEIGHT MARGIN FOR RESCUE VEHICLE TO ACCOMMODATE GUIDANCE SYSTEM AND NON-OPTIMUM MANEUVERS

- HIERARCHY OF TARGET VEHICLE OPERABLE SYSTEMS
  - ATTITUDE CONTROL
  - COMMUNICATIONS LINK (COMMAND AND TRACKING)
  - LOW LEVEL MANEUVERABILITY

- RESCUE VEHICLE SYSTEMS
  - LONG RANGE ACQUISITION RADAR
  - SHORT RANGE RF OR SCANNING LASER RADAR
  - CELESTIAL AND INERTIAL ATTITUDE SENSORS
  - AXIAL AND LATERAL THRUSTERS
  - COMMAND SEQUENCER/COMPUTER

signal during the terminal phase of rendezvous. Attitude control capability through an active command/receive link with the rescue vehicle is certainly a vital requirement for success of the final closure and docking maneuvers. Target vehicle maneuverability other than attitude control is generally not necessary since the rescue vehicle is the active rendezvous partner.

An estimate of target position knowledge error is shown in Figure 4-9 assuming conventional DSN radio tracking. The error characteristic varies linearly with geocentric tracking distance and inversely with the sine of geocentric declination. A typical range of the RMS position uncertainty is 20 to 85 km at ρ = 0.5 AU and 40 to 170 km at ρ = 1.0 AU. Sensitivity to low values of declination can be reduced significantly by using quasi very long baseline interferometry (QVLBI) techniques in addition to conventional doppler tracking. These "new" data types involving simultaneous (multi-station) doppler and range measurements are expected to be in common use for future planetary missions. Orbit transfer guidance accuracy can be made to closely approach the orbit determination knowledge accuracy by employing several midcourse correction maneuvers to nullify ΔV execution error effects. Therefore, we might reasonably expect the 3σ error at terminal rendezvous initiation not to exceed 300 km.

Radar acquisition of the target from several hundred kilometers should not present any problem to radar system design nor require excessive mass or power. Table 4-3 shows the characteristics of the rendezvous radar proposed in the Martin-Marietta study of Mars sample return missions. The design, based on technology used in the Apollo rendezvous radar, is a unified S-band PM/CW system which serves a multipurpose function for both rendezous and docking operations. It provides range, range-rate, and angle data from a maximum unambiguous range of 750 km down to a minimum docking range of 3 m. Due to rapidly degraded accuracy at very close range, range measurements are not used within 30 m of final docking; system performance relies instead on accurate range-rate and

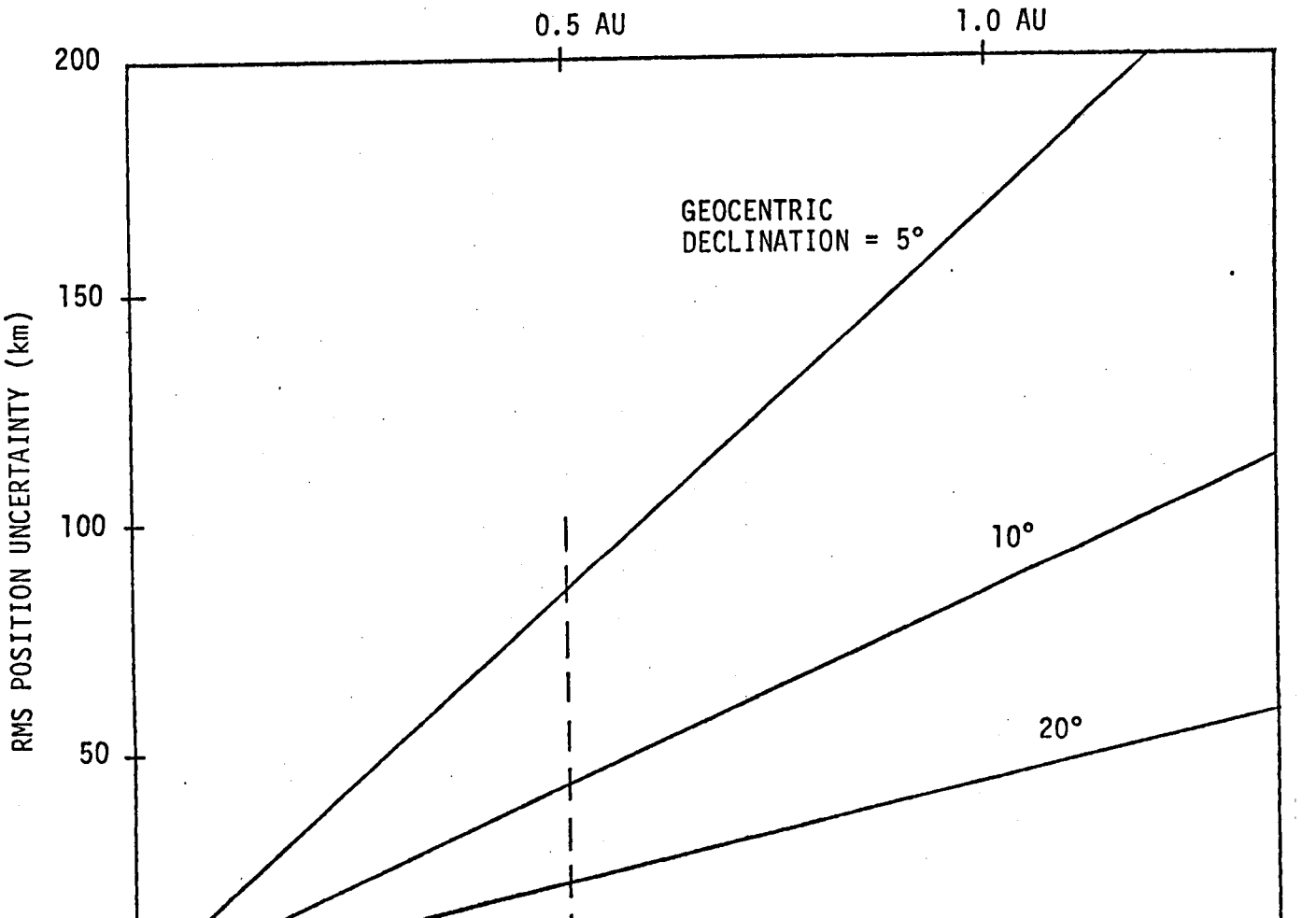

Fig. 4-9 PRELIMINARY ESTIMATE OF SPACECRAFT POSITION UNCERTAINTY AFTER SEVERAL WEEKS OF CONVENTIONAL DSN RADIO TRACKING

Table 4-3

RENDEZVOUS RADAR CHARACTERISTICS (Martin-Marietta Ref.)

System Parameters

Frequency	S-Band
Radar Type	CW
Radar Mode	Automatic
Modulation	PM (819 kc Subcarrier, 4 minor tones)
Radar Power	0.3 w (Solid State)
Maximum Range	750 km
Minimum Range	3 m
Radar Antenna	Traveling Wave Array
Angle Track Method	Phase Monopulse
Transponder Power	0.15 w (Solid State)
Transponder Antenna	Cassegrain
Coherence Ratio	220/239

Error Summary

Range Error (Bias)	3 m
Range Error (Random)	
R < 65 km	<3 m
R = 750 km	750 m
Range Rate Error (Bias)	5 cm/sec
Range Rate Error (Random)	5 cm/sec
Angle Error (Bias)	1.5 mrad
Angle Error (Random)	
R < 10 km	<0.05 mrad
R = 750 km	3.2 mrad

angle data maintained through impact. Alternative systems such as a scanning laser radar have also been proposed for short-range applications. One important advantage would be to minimize the active RF interface with the target vehicle through the use of corner reflectors instead of a transponder. Laser radar technology is currently in the breadboard stage and its future hardware development appears to be tractable. Additional sensor and control elements required on-board the rescue vehicle include celestial and inertial instrumentation for attitude control, dual-directional thrusters for axial and lateral channel trajectory control, and a command sequencer/computer to implement the autonomous maneuver strategy.

Although detailed engineering design and costing studies are clearly needed after the vehicle configurations are better defined, we would conclude that rescue mission capability is technically feasible if a cooperative rendezvous mode can be assured. Such assurance implies a limited time interval between nominal payload launch and retrieval and, perhaps, some level of redundancy in payload vehicle systems to enhance operational reliability. In the absence of cooperative rendezvous, new technology requirements are expected to be difficult to satisfy, particularly as regards capture mechanisms to implement automated docking with a massive, uncontrollable vehicle. One might consider an alternative risk reduction approach in such a circumstance--explosive destruction of the nuclear waste payload. Small remnant particles subject to erosion and ionization in the space environment can be strongly influenced by nongravitational forces such as solar radiation pressure and the solar wind. These forces tend to disperse the particle orbits and diminish the amount of material that would be intercepted by Earth. Those particles that do reenter Earth's atmosphere would most likely suffer complete burnup at high altitude into a submicron size oxide aerosol. The consequential risks of adverse health effects have been estimated to be quite small due to the extremely large dilution provided by the atmospheric volume of an entire hemisphere [2].

Section 4 References

4.1 Scofield, W. T., "A Feasibility Study of Unmanned Rendezvous and Docking in Mars Orbit," Martin-Marietta Corp. Report MCR 74-244, July 1974.

4.2 Friedlander, A. L., et al., "Analysis of Long-Term Safety Associated with Space Disposal of Hazardous Material," Science Applications, Inc., Report SAI 1-120-676-T11, December 1977.

4.3 "Space Shuttle Program Teleoperator Retrieval System," Martin-Marietta Corp., NASA Contract NAS8-32821.